



UniWeTok: An Unified Binary Tokenizer with Codebook Size 2^{128} for Unified Multimodal Large Language Model

Shaobin Zhuang^{*1,2}, Yuang Ai^{*1,3}, Jiaming Han^{*1,3}, Weijia Mao^{1,5}, Xiaohui Li²

Fangyikang Wang⁶, Xiao Wang¹, Yan Li¹, Shanchuan Lin¹, Kun Xu¹

Zhenheng Yang¹, Huaibo Huang⁴, Xiangyu Yue³, Hao Chen^{*1†‡}, Yali Wang^{7†}

¹ByteDance, ²Shanghai Jiao Tong University, ³MMLab, The Chinese University of Hong Kong

⁴Institute of Automation, Chinese Academy of Sciences, ⁵National University of Singapore

⁶Zhejiang University, ⁷Shenzhen Institutes of Advanced Technology, Chinese Academy of Sciences

*Equal contribution, †Corresponding Author, ‡Project lead

Abstract

Unified Multimodal Large Language Models (MLLMs) require a visual representation that simultaneously supports high-fidelity reconstruction, complex semantic extraction, and generative suitability. However, existing visual tokenizers typically struggle to satisfy these conflicting objectives within a single framework. In this paper, we introduce UniWeTok, a unified discrete tokenizer designed to bridge this gap using a massive binary codebook (2^{128}). For training framework, we introduce Pre-Post Distillation and a Generative-Aware Prior to enhance the semantic extraction and generative prior of the discrete tokens. In terms of model architecture, we propose a convolution-attention hybrid architecture with the SigLu activation function. SigLu activation not only bounds the encoder output and stabilizes the semantic distillation process but also effectively addresses the optimization conflict between token entropy loss and commitment loss. We further propose a three-stage training framework designed to enhance UniWeTok’s adaptability across various image resolutions and perception-sensitive scenarios, such as those involving human faces and textual content. On ImageNet, UniWeTok achieves state-of-the-art image generation performance (FID: UniWeTok 1.38 *vs.* REPA 1.42) while requiring a remarkably low training compute (Training Tokens: UniWeTok 33B *vs.* REPA 262B). On general-domain, UniWeTok demonstrates highly competitive capabilities across a broad range of tasks, including multimodal understanding, image generation (DPG Score: UniWeTok 86.63 *vs.* FLUX.1 [Dev] 83.84), and editing (GEdit Overall Score: UniWeTok 5.09 *vs.* OmniGen 5.06). We release code and models to facilitate community exploration of unified tokenizer and MLLM.

Code: <https://github.com/shallowdream204/BitDance>

1 Introduction

The success of the next-token prediction paradigm in Large Language Models (LLMs) [1, 63, 70, 71] has motivated extensive research into transferring this approach to unified vision-language modeling. However, achieving this unification presents significant challenges. A primary obstacle is the prohibitive computational

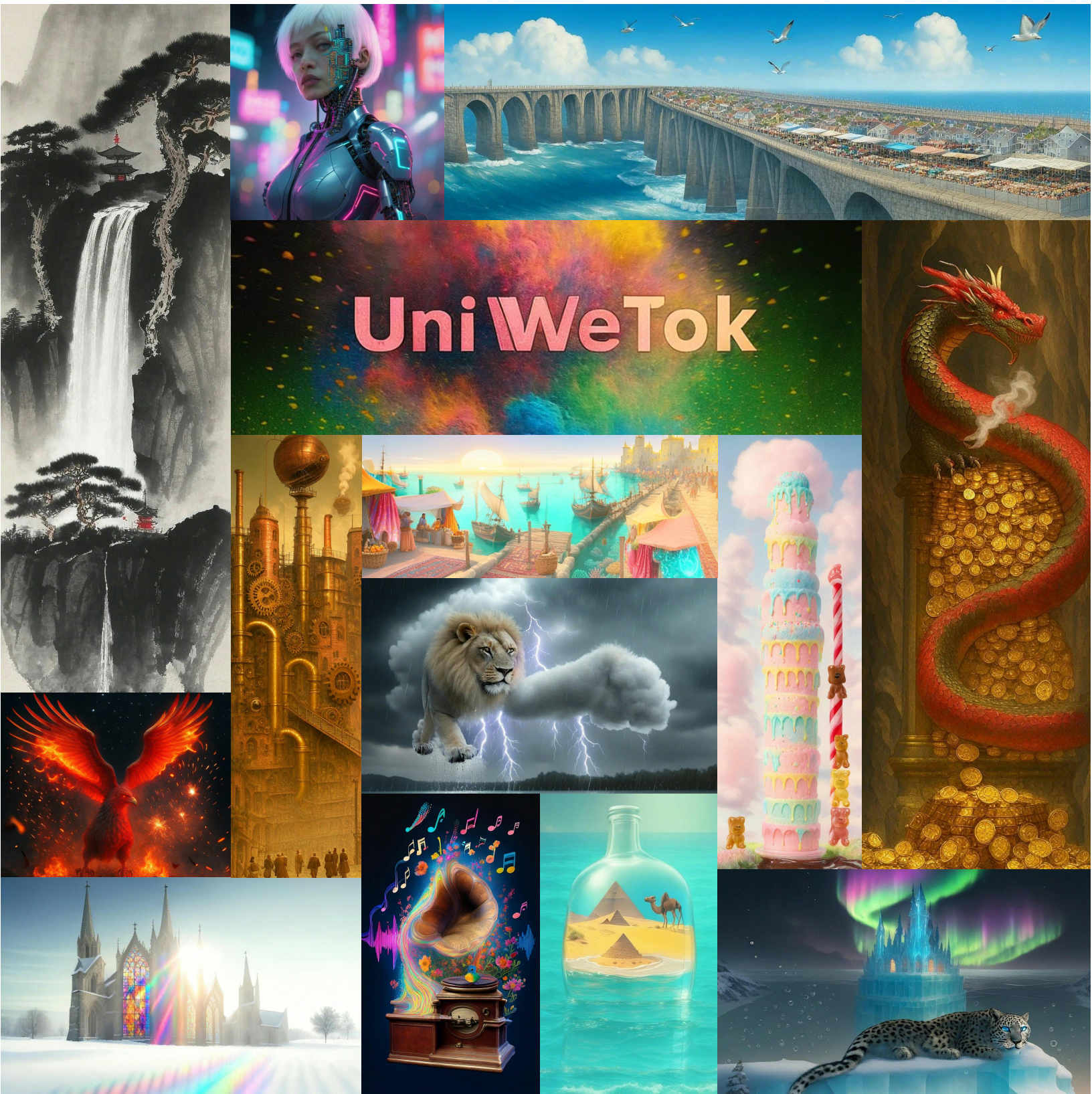


Figure 1 Various resolution samples generated by our Unified MLLM based on **UniWeTok**, showcasing its capabilities in prompt adherence, spatial reasoning, and text rendering across various artistic styles. UniWeTok employs a spatial downsampling rate of $32\times$ and a codebook size of 2^{128} , which reduces the number of visual tokens by 75% while maintaining exceptionally high reconstruction quality. Furthermore, UniWeTok possesses strong semantic extraction capabilities and generative priors, making compressed discrete visual tokens suitable for Unified Multimodal Large Language Model.

cost associated with pixel-level modeling, which necessitates effective image compression. Visual tokenizers address this by employing an encoder-decoder architecture [39] to compress images into compact latent representations for subsequent reconstruction. While employing continuous tokenizers to extract image latents is a common approach, it frequently suffers from error accumulation and mode collapse during autoregressive generation [86, 127]. Consequently, modeling the distribution of discrete tokens offers a more robust alternative.

Despite their robustness, discrete tokenizers have historically faced criticism for limited reconstruction capabilities, implying significant information loss. Recent advancements have fundamentally shifted this landscape. Through improvements to Lfq [109], BSQ [121] and GQ [127] scaled the codebook size to an unprecedented size—exceeding 2^{128} —thereby enabling individual tokens to encapsulate a massive amount of information. However, such an expansive codebook size introduces new complexities for downstream generation and understanding tasks. While recent approaches such as Infinity [31] and BitDance [3] propose solutions leveraging massive codebooks, the codebook size in text-to-image modeling remains constrained to 2^{32} . Furthermore, these approaches do not extend to multimodal understanding or the development of Unified Multimodal Large Language Models (MLLMs). This naturally leads to a question: *Is it feasible to construct a Unified MLLM based on a massive discrete visual codebook?*

To achieve this, we propose UniWeTok, a visual discrete tokenizer that unifies robust compression, semantic extraction, and generative priors into a single framework. UniWeTok maximizes token information density by achieving $32 \times$ spatial downsampling while maintaining a codebook size of 2^{128} . Building upon WeTok [127], we comprehensively advance the system across three key dimensions: (1) Training Framework: We introduce a Pre-Post Distillation (PPD) loss and a Generative-Aware Prior (GAP) loss to significantly enhance performance in downstream understanding and generation tasks. (2) Model Architecture: We propose a SigLu activation to ensure the stable convergence of the PPD loss. Furthermore, we transition to a hybrid backbone that synergizes the local inductive priors of convolutions with the global receptive field of attention mechanisms. (3) Training Pipeline: We introduce a three-stage curriculum learning strategy. By adjusting resolutions and training data distributions, we enable our UniWeTok to robustly adapt to variable resolutions and perceptually sensitive scenarios, such as human faces and text.

We first demonstrate that UniWeTok achieves state-of-the-art generation performance (FID: **UniWeTok 1.38 vs. REPA 1.42**) in class-to-image generation while incurring significantly lower training costs compared to existing methods (Training Tokens: **UniWeTok 33B vs. REPA 26B**). Building on this efficiency, our Unified MLLM based on UniWeTok not only exhibits competitive capabilities in multimodal understanding but also delivers text-to-image generation quality that surpasses the prominent open-source model (DPG Score: **UniWeTok 86.63 vs. FLUX.1 [Dev] 83.84**). Furthermore, our Unified MLLM also demonstrates remarkable proficiency in image editing (GEdit Overall Score: **UniWeTok 5.09 vs. OmniGen 5.06**). Collectively, these results rigorously validate the effectiveness of UniWeTok as the visual tokenizer for Unified MLLMs modeling.

2 Related Work

2.1 Discrete Visual Tokenizer

VQVAE [90] and VQGAN [20] employ vector-quantization (VQ) to transform visual input into discrete tokens. But they suffer from low reconstruction quality caused by instability of the codebook utilization. To overcome these drawbacks, one line of work introduces optimization strategies or modules to improve performance [41, 77, 113, 125]. Another line of work focuses on scaling up the codebook size by grouping codebooks [6, 36, 60, 117]. ImageFolder [46], DualToken [80] and TokenFlow [69] use multiple codebooks to assist in optimizing model understanding and reconstruction capabilities. However, VQ-based tokenizers still introduce additional costs due to the lookup operation [23, 41, 108]. MAGVIT-v2 [110] introduces Lookup-Free Quantization to address extra cost and proposes the entropy loss [10, 35] to ensure the utilization of the codebook. BSQ [120] assumes independence between the bits of the binary code to eliminate unbearable computational overhead from entropy loss. WeTok [126] proposes Group-Wise Lookup-Free Quantization to mitigate the codebook entropy calculation error in BSQ. However, current tokenizers based on binary codebooks barely extract any semantic information [69], and their excessively large codebooks are detrimental to downstream generation tasks [126]. In contrast, our UniWeTok successfully achieves robust semantic

extraction performance based on a binary codebook while ensuring that the extracted discrete tokens remain suitable for downstream generation.

2.2 Unified Multimodal Large Language Model

With the development of LLMs [1, 5, 63, 89], MLLMs have attracted a lot of research interest due to their strong multimodal understanding and reasoning capabilities [5, 15, 44, 52]. Beyond visual understanding, several recent works [18, 27, 83, 91, 97, 105, 124] attempt to integrate both visual understanding and generation within a unified MLLM. Emu2 [83] enables LLMs to generate CLIP embeddings, which are decoded into images using a diffusion model. Show-o [105] and Transfusion [124] integrate diffusion objectives into LLMs for image generation, but this design breaks the autoregressive paradigm and complicates the unification of the two tasks. Emu3 [93] and Chameleon [84] use VQVAE [21] as both the visual encoder and decoder, allowing unified next token prediction across images and text. Janus [13, 97] employs separate encoders for understanding and generation, resulting in distinct modalities that limit performance in multi-turn editing and interleaved generation. VILA-U [100] and UniTok [61] are trained using both pixel reconstruction and image-text alignment losses, but they struggle to converge optimally for both tasks. In contrast, we propose a discrete, semantic and generation-friendly that unifies understanding and generation within a single MLLM.

3 Method

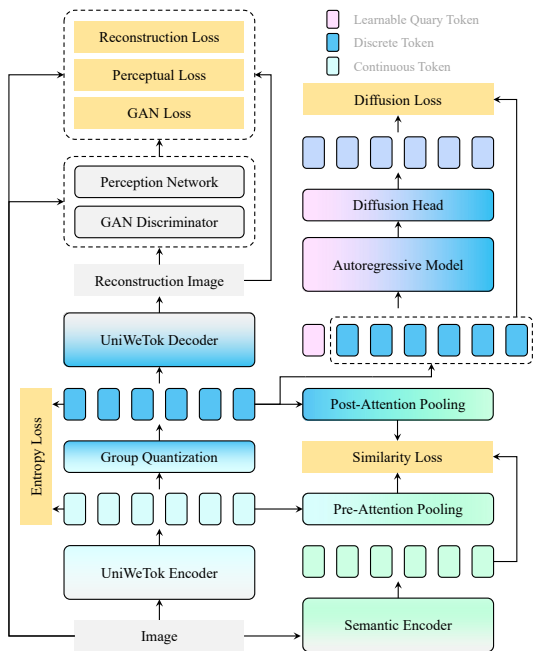


Figure 2 Illustration of UniWeTok training framework. We introduce a pre-trained semantic encoder for Pre-Post Distillation and a lightweight generative model for Generative-Aware Prior.

of WeTok consists of the following five parts,

$$\mathcal{L}_{\text{WeTok}} = \underbrace{\|\mathcal{I} - \hat{\mathcal{I}}\|^2}_{\text{Recon. Loss}} + \alpha \underbrace{\|\mathcal{U}_G - \text{sg}[\mathcal{Q}]\|^2}_{\text{Commitment Loss}} + \beta \underbrace{\mathcal{L}_{\text{LPIPS}}(\mathcal{I}, \hat{\mathcal{I}})}_{\text{Perceptual Loss}} + \gamma \underbrace{\mathcal{L}_{\text{GAN}}(\mathcal{I}, \hat{\mathcal{I}})}_{\text{GAN Loss}} + \delta \underbrace{\mathcal{L}_{\text{Entropy}}(\mathcal{U}_G, \mathcal{Q})}_{\text{Entropy Loss}}, \quad (2)$$

In this section, we present the proposed UniWeTok methodology. We begin by introducing the Pre-Post Distillation (PPD) and Generative-Aware Prior (GAP) in Sec. 3.1, which serve as the foundational elements of our training framework. Subsequently, we elaborate on the specific structural design in Sec. 3.2, focusing on the SigLu activation and the hybrid architecture. Finally, we demonstrate our three-stage curriculum training pipeline in Sec. 3.3, a critical mechanism that enables UniWeTok to generalize robustly across variable resolutions and high-sensitivity scenarios.

3.1 Training Framework

Preliminaries. WeTok [127] compress image $\mathcal{I} \in \mathbb{R}^{H \times W \times 3}$ into latent feature $\mathcal{U} = \mathcal{E}(\mathcal{I})$, $\mathcal{U} \in \mathbb{R}^{h \times w \times d}$, through the encoder \mathcal{E} . It groups the latent features in channel dimension, reshape \mathcal{U} into $\mathcal{U}_G \in \mathbb{R}^{h \times w \times g \times d'}$, where $d = gd'$ and g and d' represent the number and channel of groups. Group-Wise Lookup-Free Quantization (GQ) introduces codebooks $\mathcal{C}_{GQ,k} = \{-1, 1\}^{d'}$ to perform lookup-free quantization on each channel of latent feature,

$$Q[i, j, k, l] = \text{sign}(\mathcal{U}_G[i, j, k, l]). \quad (1)$$

Notice that we introduce $\mathcal{U}_Q = \mathcal{U}_G + \text{sg}[\mathcal{Q} - \mathcal{U}_G]$ as a variable that shares the same value as \mathcal{Q} but has a backward gradient only with respect to \mathcal{U}_G . Here, $\text{sg}[\cdot]$ denotes the stop-gradient operation. The \mathcal{U}_Q is reconstructed into image space $\hat{\mathcal{I}} = \mathcal{G}(\mathcal{U}_Q)$ through the decoder \mathcal{G} . The loss function

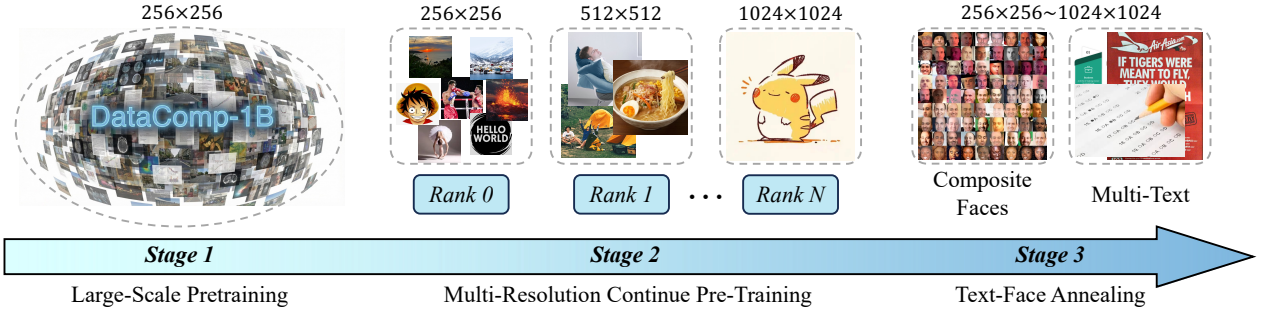


Figure 3 Illustration of the three-stage training pipeline of UniWeTok.

where perceptual loss [119] and GAN loss are introduced for better visual quality. Entropy loss consists of token entropy loss and codebook entropy loss. The specific form of token entropy loss is as follows:

$$\mathcal{L}_{\text{Token Entropy}} = \frac{1}{hw} \sum_{i=1}^h \sum_{j=1}^w \sum_{k=1}^g H(q_G(\mathbf{c}_k | \mathcal{U}_G[i, j, k])), \quad (3)$$

where $q_G(\mathbf{c}_k | \mathcal{U}_G[i, j, k])$ denote the conditional distribution of $\mathbf{c}_k \in \mathcal{C}_{GQ,k}$ given $\mathcal{U}_G[i, j, k]$.

Pre-Post Distillation. To facilitate the effective application of UniWeTok in multimodal understanding tasks, it is imperative to endow the encoder with semantic extraction capabilities. As illustrated in Fig. 2, we employ a pre-trained semantic encoder E_T as the teacher for distillation. Specifically, the teacher encodes the input image \mathcal{I} into semantic latents $f_t = E_T(\mathcal{I})$, $f_t \in \mathbb{R}^{1 \times d_T}$, where d_T is the output dimension of E_T . We employ cosine similarity loss for distillation. Notably, we align both \mathcal{U}_G and \mathcal{U}_Q with f_T ,

$$\mathcal{L}_{\text{Pre Distill}} = 1 - \frac{u_G \cdot f_T}{\|u_G\| \|f_T\|}, \quad u_G = \text{AttnPool}_{\text{Pre}}(\mathcal{U}_G), \quad (4)$$

$$\mathcal{L}_{\text{Post Distill}} = 1 - \frac{u_Q \cdot f_T}{\|u_Q\| \|f_T\|}, \quad u_Q = \text{AttnPool}_{\text{Post}}(\mathcal{U}_Q), \quad (5)$$

$$\mathcal{L}_{\text{PPD}} = \mathcal{L}_{\text{Pre Distill}} + \eta \mathcal{L}_{\text{Post Distill}}. \quad (6)$$

This alignment strategy serves to enhance the semantic extraction capability, ensuring that the model effectively captures the underlying semantic information.

Generative-Aware Prior. Increasing the number of groups significantly enhances the reconstruction performance of the discrete tokenizer [127]. However, this improvement comes at the cost of increased difficulty for downstream generation tasks. To mitigate this issue, we inject a Generative-Aware Prior, enabling the model to perceive the generation objective during the training phase. As illustrated in Fig. 2, we flatten the \mathcal{U}_Q into 1D sequence $\mathcal{U}_B \in \mathbb{R}^{(h \times w) \times d}$ and feed it into a randomly initialized tiny BitDance [3] model B to perform a next-token diffusion task, which is supervised using the MSE loss,

$$\mathcal{L}_{\text{GAP}} = \mathbb{E}_{\epsilon \in \mathcal{N}(\mathbf{0}, \mathbf{I})} \|\mathcal{U}_B - B([\text{Query}, \mathcal{U}_B[:, -1]], \epsilon, t)\|^2, \quad (7)$$

where t is random sampled from $[0, 1]$. Query token allows the model not to miss the prediction of the first token and learn the distribution of the entire sequence.

Consequently, the comprehensive loss function for the UniWeTok framework is defined as follows:

$$\mathcal{L}_{\text{UniWeTok}} = \mathcal{L}_{\text{WeTok}} + \theta \mathcal{L}_{\text{PPD}} + \mu \mathcal{L}_{\text{GAP}}, \quad (8)$$

where θ and μ serve as hyperparameters that to regulate the weight of reconstruction, understanding and generation task during the UniWeTok training process.



Figure 4 Ablation study of three-stage training pipeline.

3.2 Unified Discrete Tokenizer Architecture

Hybrid backbone. UniWeTok employs a hybrid architecture for both encoder and decoder. In the encoder, input images are initially processed by stacked residual blocks, which serve to extract low-level information and perform spatial downsampling. This is followed by a sequence of transformer blocks designed to capture global context. The decoder mirrors this structure symmetrically. As shown in Tab. 7, this design effectively integrates the local inductive bias of convolutional layers while minimizing the computational overhead associated with the attention mechanism. Notably, the original WeTok architectu utilizes a downsample block

that executes spatial downsampling before channel expansion, a sequential process that results in information loss. To address this, we modify the downsample block to perform channel expansion concurrently with downsampling. As shown in Tab. 4, this modification yields a substantial improvement in the reconstruction capabilities.

SigLu activation. During the training process, we observe a notable phenomenon. As shown in Tab. 2, when we perform semantic distillation exclusively on \mathcal{U}_Q , the model fails to capture meaningful semantic information. We attribute this issue to the commitment loss, which rigidly anchors the encoder outputs \mathcal{U}_G to values near -1 or 1, making it difficult for the model to adapt its semantic representations. This constraint also creates a fundamental conflict with the token entropy loss, as the latter drives the \mathcal{U}_G towards negative or positive infinity. To resolve this optimization conflict, we propose the SigLu activation function,

$$\text{SigLu}(x) = \frac{1 - e^x}{1 + e^x}, \quad (9)$$

where SigLu is integrated as the final layer of the encoder. The SigLu activation inherently constrains \mathcal{U}_G to the interval $[-1, 1]$. Under this condition, the token entropy loss becomes equivalent to the commitment loss. Consequently, we set $\alpha=0$ in Eq. 2, effectively replacing the commitment term with the token entropy loss. As shown in Tab. 2, SigLu enables the model to perform semantic distillation stably. The specific model architecture could be seen in App. A.

3.3 Training Pipeline

As illustrated in Fig. 4, our UniWeTok model is constrained to the specific image resolution defined during its pre-training. However, practical downstream applications inevitably require handling a diverse range of resolutions. To bridge this gap, we propose a three-stage progressive pre-training strategy. As depicted in Fig. 3, the first stage prioritizes computational efficiency by performing large-scale pre-training on a general-domain dataset at a fixed resolution of 256×256 . In the second stage, we partition computational resources to facilitate training across multiple resolutions simultaneously. Finally, the third stage employs an annealing training phase focused on perceptually sensitive domains, such as faces and text. This progressive refinement ensures that UniWeTok is optimally aligned with complex downstream understanding and generation tasks.

4 Experiments

Datasets. We train on two datasets: (i) ImageNet [75] training set; and (ii) the general-domain dataset DataComp-1B [25]. For evaluations on ImageNet, we measure the reconstruction (rFID [32], PSNR, SSIM [95], and LPIPS [119]) and semantic extraction (zero-shot classification [72]) performance on the ImageNet 50k validation set as well as the generation performance of the generative model (gFID, IS, Precision, and Recall). Regarding general-domain, we evaluate the reconstruction performance on the ImageNet 50k validation set and the MS-COCO 2017 validation set [50]. To comprehensively assess the capabilities of UniWeTok in downstream scenarios, we train a Unified MLLM based on UniWeTok and evaluate its performance on downstream understanding (SEEDB [42], POPE [47], VQAv2 [30], GQA [34], SQA [57], TQA [79], CQA [64], AI2D [37], RWQA [101], MMMU [116], MME [24]), generation (GenEval [29], DPG-Bench [33]) and editing benchmarks (GEdit [56]). Unless otherwise stated, we conduct ablation studies on the ImageNet training set.

Settings. UniWeTok adopts the architecture proposed in WeTok [127] with a downsampling factor of 32 and a codebook size of 2^{128} . Images are randomly cropped to target sizes for training. For ablation study, all models are trained for 250K steps with Adam [38] and a consistent set of hyperparameters. For large-scale training, hyperparameters are individually tuned for each model to achieve optimal performance. For class-to-image generation and Unified MLLM, we adopt the model architecture and training setting in BitDance [3].

4.1 Ablation Studies

Training loss. We conduct ablation studies on the WeTok loss, the semantic distillation loss, and the prior loss. As shown in Tab. 1, incorporating the semantic distillation loss significantly enhances the semantic extraction capability of the tokenizer. Furthermore, the introduction of the prior loss improves the tokenizer’s

performance on downstream generation while maintaining its reconstruction capability. Unexpectedly, the prior loss not only preserves the model’s understanding capability but actually enhances it.

Table 1 Ablation study of semantic distillation and prior loss. We ablate the contribution of each loss.

Setting		Gen. gFID↓	Reconstruction					Zero-shot Acc (%)		
PPD	GAP		rFID↓	PSNR↑	SSIM↑	LPIPS(A)	LPIPS(V)	Top-1	Top-5	Top-10
✗	✗	2.38	1.33	22.67	0.66	0.11	0.20	-	-	-
✓	✗	2.66	1.12	22.32	0.65	0.12	0.21	46.89	73.66	81.11
✓	✓	2.35	1.18	22.27	0.63	0.12	0.22	48.77	75.62	83.84

SigLu activation. As shown in Tab. 2, the GQ poses a significant challenge for semantic extraction. Post distillation almost fails to converge. Pre distillation stabilizes convergence, while it fails to ensure semantics in the discrete latents. Our proposed SigLu activation constrains the feature space, enabling effective post distillation.

Table 2 SigLu activation ablation. SigLu activation makes post-distillation effective.

Method	Top-1	Top-5	Top-10
Pre Distill	55.26	79.55	85.52
Post Distill	0.10	0.53	0.95
SigLu + Post	41.51	69.51	77.73

Table 3 Pre-Post Distillation ablation. Pre-Post yields the best performance.

Distillation Loss		Zero-shot Acc (%)		
PRE	POST	Top-1	Top-5	Top-10
✓	✗	0.10	0.52	1.01
✗	✓	41.51	69.51	77.73
✓	✓	51.32	76.70	83.26

Pre-Post Distillation. As shown in Tab. 3, we demonstrate the effectiveness of our pre-post distillation strategy. The combination of pre and post distillation yields the best performance, reaching 51.32% zero-shot Top-1 accuracy.

Bottleneck channel. As shown in Tab. 4, we ablate channel widths of the bottlenecks. Doubling the channel significantly lowers rFID (from 1.58 to 1.12) and improves semantic accuracy by over 7%, proving that a wider bottleneck is essential for visual compression and semantic extraction.

Table 4 Bottleneck channel ablation. Extending channel width of bottleneck significantly improves reconstruction fidelity and semantic extraction capability.

Setting	Reconstruction					Zero-shot Acc (%)		
	rFID↓	PSNR↑	SSIM↑	LPIPS(A)	LPIPS(V)	Top-1	Top-5	Top-10
Single Channel	1.58	21.89	0.63	0.13	0.23	39.45	68.00	76.77
Double Channel	1.12	22.32	0.65	0.12	0.21	46.89	73.66	81.11

Generative-Aware Prior. Tab. 5 shows that while reconstruction metrics remain stable, generative quality (gFID) improves notably from 2.66 to 2.38 with GAP and Query token, confirming that regularizing the latent space benefits downstream generation task.

Table 5 Generative-Aware Prior ablation.

Method	Gen.	gFID↓	Reconstruction					Zero-shot Acc (%)		
			rFID↓	PSNR↑	SSIM↑	LPIPS(A)	LPIPS(V)	Top-1	Top-5	Top-10
✗	✗	2.66	1.12	22.32	0.65	0.12	0.21	46.89	73.66	81.11
✓	✗	3.89	1.16	22.11	0.63	0.13	0.22	48.47	74.80	82.23
✓	✓	2.38	1.18	22.27	0.63	0.12	0.22	48.77	75.62	83.84

Training configurations on DataComp-1B. Tab. 6 shows that attention head is better than linear head. Moreover, scaling the batch size tripling the zero-shot accuracy.

Table 6 Training configuration ablations on DataComp-1B. Attention-based semantic head and large batch size are critical for model convergence on general-domain dataset.

Setting	Reconstruction					Zero-shot Acc (%)		
	rFID ↓	PSNR ↑	SSIM ↑	LPIPS(A)	LPIPS(V)	Top-1	Top-5	Top-10
<i>Semantic Head Architecture</i>								
Linear Head	2.91	21.96	0.63	0.13	0.24	3.89	13.85	21.93
Attention Head	3.10	22.02	0.63	0.13	0.24	4.09	14.39	23.31
<i>Training Batch Size</i>								
Batch Size 128	3.10	22.02	0.63	0.13	0.24	4.09	14.39	23.31
Batch Size 1024	1.75	22.56	0.65	0.12	0.22	11.69	31.38	43.34

Hybrid architecture. On Datacomp-1B, Tab. 7 validates our hybrid backbone. CNNs excel at texture (rFID 1.75) but lack semantics, while Transformers capture semantics (Top-1 26.09%) but struggle with detail. Our hybrid design achieves the best of both worlds (rFID 1.35, Top-1 35.41%).

Table 7 Architecture ablation. The hybrid backbone successfully synergizes the local inductive bias of convolution with the global understanding capability of attention.

Backbone	Reconstruction					Zero-shot Acc (%)		
	rFID ↓	PSNR ↑	SSIM ↑	LPIPS(A)	LPIPS(V)	Top-1	Top-5	Top-10
CNN Only	1.75	22.56	0.65	0.12	0.22	11.69	31.38	43.34
Transformer Only	3.38	22.02	0.65	0.14	0.26	26.09	52.77	64.28
Hybrid (Ours)	1.35	22.54	0.66	0.13	0.22	35.41	63.91	73.50

Three-stage training pipeline. As shown in Fig. 4, compared to stage 1, the model trained in stage 2 supports variable-resolution image reconstruction. Furthermore, the model trained in stage 3 demonstrates significantly improved performance in processing faces and text.

Implementation details could be found in App. B.

4.2 Comparison with State-of-the-Art

Visual Generation on ImageNet. We first evaluate the reconstruction performance of UniWeTok on the ImageNet 50K validation dataset. As shown in Tab. 8, UniWeTok compresses a 256×256 resolution image into only **64 tokens**, which represents a **75%** reduction in token count compared to other mainstream tokenizers. Following the BitDance setting, we employ UniWeTok as the visual tokenizer for autoregressive modeling. As shown in Tab. 9, UniWeTok-H achieves a state-of-the-art FID of **1.38**. Remarkably, our model requires training on only **33B** tokens and generates just 64 tokens during inference, significantly outperforming various models that demand extensive training scales and incur higher computational costs during inference.

Unified MLLM. We first compared the reconstruction performance of tokenizers trained on general-domain dataset. As shown in Tab. 10, our UniWeTok outperforms most state-of-the-art general tokenizers in reconstruction performance while utilizing only **25%** of the visual token count. This reduction in sequence length allows for larger batch sizes in the subsequent training of unified MLLMs, significantly enhancing training efficiency. Given UniWeTok’s capability to support image compression and reconstruction at variable resolutions, we employ **native resolutions** for Unified MLLM training. This ensures that the inherent spatial information of the data is preserved without the distortions introduced by resizing or cropping. Following Emu3, after unified pretraining, we finetune the Unified MLLM into UniWeTok-Gen, UniWeTok-Edit and UniWeTok-Chat for better downstream performance. As shown in Tab. 11, UniWeTok-Gen demonstrates superior performance on image generation benchmarks, outperforming various diffusion-based models. As shown in Tab. 12, UniWeTok-Chat presents competitive understanding performance across a broad range

Table 8 Reconstruction evaluation on 256×256 ImageNet 50K validation set. All models are trained on ImageNet. UniWeTok achieves SOTA results with $32 \times$ downsampling ratio.

Method	Tokens \downarrow	Ratio \uparrow	Codebook Size	rFID \downarrow	PSNR \uparrow	Codebook Usage \uparrow
VQGAN [19]	16×16	16	16384	4.99	20.00	—
SD-VQGAN [74]	16×16	16	16384	5.15	—	—
MaskGIT [10]	16×16	16	1024	2.28	—	—
ReVQ [117]	16×16	16	65536	2.57	21.69	—
LlamaGen [81]	16×16	16	16384	2.19	20.79	97%
ReVQ [117]	16×16	16	2^{18}	2.05	21.96	—
TiTok [112]	256	16	4096	1.66	20.01	100%
FlexTok [4]	256	16	64000	1.45	18.53	—
VAR [87]	16×16	16	4096	—	21.30	97%
IBQ [78]	16×16	16	16384	1.37	22.35	96%
Open-MAGVIT2 [58]	16×16	16	2^{18}	1.17	22.64	100%
IBQ [78]	16×16	16	2^{18}	1.00	20.30	84%
FlowMo-Lo [76]	256	16	2^{18}	0.95	22.07	—
VFMTok [123]	256	16	16384	0.89	—	100%
GigaTok [106]	256	16	16384	0.79	21.65	—
AliTok [98]	273	15.5	4096	0.84	—	—
UniWeTok (Ours)	8×8	32	2^{128}	0.79	23.26	100%

Table 9 Comparison of class-conditional image generation on ImageNet 256 \times 256. UniWeTok achieves superior performance while employing standard causal autoregressive modeling.

Method	Train Tokens \downarrow	Infer Tokens \downarrow	#Params	FID \downarrow	IS \uparrow	Pre. \uparrow	Rec. \uparrow
<i>Continuous Tokens</i>							
DiT-XL/2 [67]	459B	256	675M	2.27	278.2	0.83	0.57
SiT-XL/2 [62]	459B	256	675M	2.06	277.5	0.83	0.59
MDTv2 [26]	131B	256	675M	1.58	314.7	0.79	0.65
REPA [115]	262B	256	675M	1.42	305.7	0.80	0.65
MAR-B [45]	262B	256	208M	2.31	281.7	0.82	0.57
MAR-L [45]	262B	256	479M	1.78	296.0	0.81	0.60
MAR-H [45]	262B	256	943M	1.55	303.7	0.81	0.62
NiT-XL [96]	197B	64	675M	2.03	265.26	0.80	0.62
<i>Discrete Tokens</i>							
LlamaGen-L [82]	98M	256	343M	3.07	256.1	0.83	0.52
LlamaGen-XL [82]	98M	256	775M	2.62	244.1	0.80	0.57
LlamaGen-XXL [82]	98M	256	1.4B	2.34	253.9	0.80	0.59
RandAR-L [66]	98M	256	343M	2.55	288.8	0.81	0.58
RandAR-XL [66]	98M	256	775M	2.22	314.2	0.80	0.60
RandAR-XXL [66]	98M	256	1.4B	2.15	322.0	0.79	0.62
RAR-L [114]	131M	256	461M	1.70	299.5	0.81	0.60
RAR-XL [114]	131M	256	955M	1.50	306.9	0.80	0.62
RAR-XXL [114]	131M	256	1.5B	1.48	326.0	0.80	0.63
OpenMAGVIT2-XL [59]	115M	256	1.5B	2.33	271.8	0.84	0.54
MAGVIT-v2 [109]	88M	256	307M	1.78	319.4	-	-
VAR-d20 [88]	82M	256	600M	2.57	302.6	0.83	0.56
VAR-d30 [88]	115M	256	2B	1.92	323.1	0.82	0.59
WeTok-AR-XL [127]	328M	256	1.5B	2.31	276.6	0.84	0.55
UniWeTok-B	33B	64	242M	2.35	284.47	0.80	0.59
UniWeTok-L	33B	64	527M	1.68	288.56	0.80	0.62
UniWeTok-H	33B	64	1.0B	1.38	284.34	0.80	0.63

Table 10 Zero-shot reconstruction comparison on ImageNet and MS-COCO val2017 validation set. Our UniWeTok achieves the best performance on different resolution settings.

Method	Ratio \downarrow	MS-COCO 2017			Imagenet-1k		
		rFID \downarrow	PSNR \uparrow	SSIM \uparrow	rFID \downarrow	PSNR \uparrow	SSIM \uparrow
<i>Resize 256 × 256</i>							
Cosmos [2]	16	11.97	19.22	0.48	4.57	19.93	0.49
Show-o [104]	16	9.26	20.90	0.59	3.50	21.34	0.59
WeTok [127]	32	8.94	20.31	0.55	3.49	20.77	0.55
Open-MAGVIT2-I-PT [58]	16	7.93	22.21	0.62	2.55	22.21	0.62
LlamaGen [81]	16	8.40	20.28	0.55	2.47	20.65	0.54
WeTok [127]	16	6.55	21.99	0.63	1.58	22.38	0.62
BSQ [121]	16	-	-	-	3.81	24.12	0.66
QLIP-B [122]	16	-	-	-	3.21	23.16	0.63
QLIP-L [122]	14	-	-	-	1.46	25.36	0.69
TokenFlow [122]	16	-	-	-	1.37	21.41	0.69
UniWeTok (Ours)	32	6.18	22.58	0.66	1.18	22.97	0.66
<i>Original Resolution</i>							
WeTok [127]	32	8.94	20.31	0.55	3.49	20.77	0.55
Cosmos [2]	16	7.23	20.45	0.53	2.52	20.49	0.52
Open-MAGVIT2-I-PT [58]	16	6.65	21.61	0.57	1.39	21.74	0.56
SD-VAE 1.x [73]	8	5.94	21.68	0.64	1.35	21.99	0.63
WeTok [127]	16	5.30	21.94	0.59	0.81	21.99	0.58
UniWeTok (Ours)	32	6.46	22.29	0.65	1.25	22.66	0.65

of benchmarks. In Tab. 13, UniWeTok-Edit surpasses the diffusion model on the image editing task as an autoregressive model at a similar parameter scale for the first time. The visualization results can be seen in Fig. 1,7,8,9.

Table 11 Comparisons of visual generation quality on GenEval and DPG-Bench.

Method	# Params	GenEval [29]						DPG-Bench [33]					
		Single Obj.	Two Obj.	Counting	Colors	Position	Color Attr.	Overall \uparrow	Global	Entity	Attribute	Relation	Other
<i>Diffusion-based Model</i>													
SDV1.5 [73]	0.9B	0.97	0.38	0.35	0.76	0.04	0.06	0.43	74.63	74.23	75.39	73.49	67.81
PixArt- α [12]	0.6B	0.98	0.50	0.44	0.80	0.08	0.07	0.48	74.97	79.32	78.60	82.57	76.96
SDV2.1 [73]	0.9B	0.98	0.51	0.44	0.85	0.07	0.17	0.50	-	-	-	-	71.11
SDXL [68]	2.6B	0.98	0.74	0.39	0.85	0.15	0.23	0.55	83.27	82.43	80.91	86.76	80.41
Playground v2.5 [43]	2.6B	-	-	-	-	-	-	-	83.06	82.59	81.20	84.08	83.50
Hunyuan DiT [48]	1.5B	-	-	-	-	-	-	-	84.59	80.59	88.01	74.36	86.41
PixArt- Σ [11]	0.6B	-	-	-	-	-	-	-	86.89	82.89	88.94	86.59	87.68
DALLE3 [8]	-	0.96	0.87	0.47	0.83	0.43	0.45	0.67	90.97	89.61	88.39	90.58	89.83
SD3-Medium [22]	2B	0.99	0.94	0.72	0.89	0.33	0.60	0.74	87.90	91.01	88.83	80.70	88.68
SANA-1.5 [103]	4.8B	0.99	0.93	0.86	0.84	0.59	0.65	0.81	-	-	-	-	84.70
<i>Autoregressive-based Model</i>													
Chameleon [85]	7B	-	-	-	-	-	-	0.39	-	-	-	-	-
LlamaGen [45]	0.8B	0.71	0.34	0.21	0.58	0.07	0.04	0.32	81.76	75.43	76.17	84.76	58.40
EMU3-Gen [94]	8B	0.98	0.71	0.34	0.81	0.17	0.21	0.54	85.21	86.68	86.84	90.22	83.15
TokenFlow [69]	13B	0.97	0.66	0.40	0.84	0.17	0.26	0.55	78.72	79.22	81.29	85.22	71.20
Janus [97]	1.3B	0.97	0.68	0.30	0.84	0.46	0.42	0.61	82.33	87.38	87.70	85.46	86.41
SimpleAR [92]	1.5B	-	0.90	-	-	0.28	0.45	0.63	87.97	-	-	86.33	-
Transfusion [124]	7B	-	-	-	-	-	-	0.63	-	-	-	-	-
NextStep-1 [86]	14B	-	-	-	-	-	-	0.73	-	-	-	-	85.28
Harmon [99]	1.5B	0.99	0.86	0.66	0.85	0.74	0.48	0.76	-	-	-	-	-
Infinity [31]	8B	-	-	-	-	-	-	0.79	-	-	-	-	86.6
Janus-Pro [13]	7B	0.99	0.89	0.59	0.90	0.79	0.66	0.80	86.90	88.90	89.40	89.32	89.48
UniWeTok-Gen (Ours)	8B	0.99	0.94	0.43	0.90	0.78	0.81	0.81	87.54	91.99	90.72	92.92	91.11

Table 12 Comparison on multimodal understanding benchmarks.

Method	Pretrained-LLM	SEEDB	POPE	VQAv2	GQA	SQA	TQA	CQA	AI2D	RWQA	MMMU	MME-P	MME-S
Understanding Only Model													
InstructBLIP [15]	Vicuna-7B	53.4	—	—	49.2	60.5	50.1	12.5	33.8	37.4	30.6	1212.8	—
IDEFICS-9B [40]	LLaMA-7B	—	—	50.9	38.4	—	25.9	—	42.2	42.1	18.4	—	—
LLaVA-1.5 [53]	Vicuna-7B	64.3	85.9	78.5	62.0	66.8	46.1	18.2	54.8	54.8	35.3	1510.7	—
InternVL-Chat [14]	Vicuna-7B	—	86.4	79.3	62.9	—	57.0	—	—	—	—	1298.5	—
mPLUG-Owl2 [107]	LLaMA2-7B	57.8	86.2	79.4	56.1	68.7	58.2	22.8	55.7	50.3	32.7	—	—
LLaVA-1.6(HD) [54]	Vicuna-7B	64.7	86.5	81.8	64.2	70.2	64.9	54.8	66.6	57.8	35.1	—	1778.0
VILA [49]	LLaMA2-7B	61.1	85.5	80.8	63.3	73.7	66.6	—	—	—	—	1533.0	—
Unified Model													
Fuyu-8B(HD) [7]	Persimmon-8B	—	74.1	74.2	—	—	—	—	64.5	—	27.9	—	—
Chameleon-MT-34B [85]	—	—	—	69.6	—	—	—	—	—	—	—	—	—
LWM-7B [51]	—	—	75.2	55.8	44.8	47.7	—	—	—	—	—	—	—
Show-o [104]	Phi-1.5-1.3B	—	73.8	59.3	48.7	—	—	—	—	—	25.1	1097.2	—
VILA-U [100]	LLaMA2-7B	56.3	83.9	75.3	58.3	—	48.3	—	—	—	—	1336.2	—
Harmon [100]	Qwen2.5-1.5B	67.1	87.6	—	58.9	—	—	—	—	—	38.9	1155.0	1476.0
EVE-7B(HD) [17]	Vicuna-7B	56.8	85.0	78.6	62.6	64.9	56.8	—	—	—	—	1305.7	—
Emu3-Chat [94]	—	68.2	85.2	75.1	60.3	89.2	64.7	68.6	70.0	57.4	31.6	—	—
TokenFlow-L [60]	Vicuna-13B	62.6	85.0	73.9	60.3	—	54.1	—	56.6	49.2	34.4	1365.4	1622.9
UniTok [60]	LLaMA-2-7B	—	83.2	61.1	—	—	51.6	—	—	—	—	1448.0	—
UniWeTok-Chat	Qwen3-8B	69.3	85.6	75.8	63.1	80.3	53.7	65.1	73.9	54.8	40.0	1415.7	1796.6

Table 13 Comparison on GEdit-Bench. G_SC, G_PQ, and G_O refer to the metrics evaluated by GPT-4.1.

Model	GEdit-EN (Full set)			GEdit-CN (Full set)		
	G_SC↑	G_PQ↑	G_O↑	G_SC↑	G_PQ↑	G_O↑
<i>Private</i>						
Gemini 2.0 [28]	6.73	6.61	6.32	5.43	6.78	5.36
GPT-4o [65]	7.85	7.62	7.53	7.67	7.56	7.30
<i>Open-Source Diffusion</i>						
Instruct-Pix2Pix [9]	3.58	5.49	3.68	-	-	-
MagicBrush [118]	4.68	5.66	4.52	-	-	-
AnyEdit [111]	3.18	5.82	3.21	-	-	-
OmniGen [102]	5.96	5.89	5.06	-	-	-
Step1X-Edit [55]	7.09	6.76	6.70	7.20	6.87	6.86
BAGEL [16]	7.36	6.83	6.52	7.34	6.85	6.50
<i>Open-Source Autoregressive</i>						
UniWeTok-Edit	5.86	5.89	5.09	5.78	5.92	5.11

5 Conclusion

We presented UniWeTok, a unified discrete tokenizer designed to resolve the conflict between high-fidelity reconstruction, multimodal understanding and generation. By integrating a convolution-attention hybrid backbone with the SigLu activation function, UniWeTok successfully incorporates Pre-Post Distillation and Generative-Aware Prior, allowing a unified discrete tokenizer with massive codebook size 2^{128} to extract semantic concepts, fine-grained texture details, and generative prior effectively. Our UniWeTok establishes a robust and efficient baseline for future Unified MLLM works, suggesting that a single, well-optimized tokenizer is sufficient to address the complex challenges inherent in Unified MLLMs.

References

- [1] Josh Achiam, Steven Adler, Sandhini Agarwal, Lama Ahmad, Ilge Akkaya, Florencia Leoni Aleman, Diogo Almeida, Janko Altenschmidt, Sam Altman, Shyamal Anadkat, et al. Gpt-4 technical report. [arXiv preprint arXiv:2303.08774](https://arxiv.org/abs/2303.08774), 2023.
- [2] Nvidia Niket Agarwal, Arslan Ali, Maciej Bala, Yogesh Balaji, Erik Barker, Tiffany Cai, Prithvijit Chattopadhyay, Yongxin Chen, Yin Cui, Yifan Ding, Daniel Dworakowski, Jiaojiao Fan, Michele Fenzi, Francesco Ferroni, Sanja Fidler, Dieter Fox, Songwei Ge, Yunhao Ge, Jinwei Gu, Siddharth Gururani, Ethan He, Jiahui Huang, Jacob Samuel Huffman, Pooya Jannaty, Jingyi Jin, Seung Wook Kim, Gergely Kl'ar, Grace Lam, Shiyi Lan, Laura Leal-Taixé, Anqi Li, Zhaoshuo Li, Chen-Hsuan Lin, Tsung-Yi Lin, Huan Ling, Ming-Yu Liu, Xian Liu, Alice Luo, Qianli Ma, Hanzi Mao, Kaichun Mo, Arsalan Mousavian, Seungjun Nah, Sriharsha Niverty, David Page, Despoina Paschalidou, Zeeshan Patel, Lindsey Pavao, Morteza Ramezanali, Fitsum A. Reda, Xiao-Shuai Ren, Vasanth Rao Naik Sabavat, Ed Schmerling, Stella Shi, Bartosz Stefaniak, Shitao Tang, Lyne P. Tchapmi, Przemek Tredak, Wei-Cheng Tseng, Jibin Rajan Varghese, Hao Wang, Haoxiang Wang, Hengyi Wang, Tingwei Wang, Fangyin Wei, Xinyue Wei, Jay Zhangjie Wu, Jiashu Xu, Wei Yang, Lin Yen-Chen, Xiaohui Zeng, Yuan Zeng, Jing Zhang, Qinsheng Zhang, Yuxuan Zhang, Qingqing Zhao, and Artur Zolkowski. Cosmos world foundation model platform for physical ai. [ArXiv](https://arxiv.org/abs/2501.03575), abs/2501.03575, 2025.
- [3] Yuang Ai, Jiaming Han, Shaobin Zhuang, Xuefeng Hu, Ziyan Yang, Zhenheng Yang, Huaibo Huang, Xiangyu Yue, and Hao Chen. Bitdance: Scaling autoregressive generative models with binary tokens, 2026. URL <https://github.com/shallowdream204/BitDance>.
- [4] Roman Bachmann, Jesse Allardice, David Mizrahi, Enrico Fini, Oğuzhan Fatih Kar, Elmira Amirloo, Alaaeldin El-Nouby, Amir Zamir, and Afshin Dehghan. Flextok: Resampling images into 1d token sequences of flexible length. In *Forty-second International Conference on Machine Learning*, 2025.
- [5] Jinze Bai, Shuai Bai, Yunfei Chu, Zeyu Cui, Kai Dang, Xiaodong Deng, Yang Fan, Wenbin Ge, Yu Han, Fei Huang, et al. Qwen technical report. [arXiv preprint arXiv:2309.16609](https://arxiv.org/abs/2309.16609), 2023.
- [6] Zechen Bai, Jianxiong Gao, Ziteng Gao, Pichao Wang, Zheng Zhang, Tong He, and Mike Zheng Shou. Factorized visual tokenization and generation. [ArXiv](https://arxiv.org/abs/2411.16681), abs/2411.16681, 2024. URL <https://api.semanticscholar.org/CorpusID:274281440>.
- [7] Rohan Bavishi, Erich Elsen, Curtis Hawthorne, Maxwell Nye, Augustus Odena, Arushi Somani, and Sağnak. Taşırlar. Introducing our multimodal models., 2023. URL <https://www.adept.ai/blog/fuyu-8b>.
- [8] James Betker, Gabriel Goh, Li Jing, Tim Brooks, Jianfeng Wang, Linjie Li, Long Ouyang, Juntang Zhuang, Joyce Lee, Yufei Guo, et al. Improving image generation with better captions. [Computer Science](https://cdn.openai.com/papers/dall-e-3.pdf). <https://cdn.openai.com/papers/dall-e-3.pdf>, 2(3):8, 2023.
- [9] Tim Brooks, Aleksander Holynski, and Alexei A. Efros. Instructpix2pix: Learning to follow image editing instructions. In *CVPR*, 2023.
- [10] Huiwen Chang, Han Zhang, Lu Jiang, Ce Liu, and William T. Freeman. Maskgit: Masked generative image transformer. *2022 IEEE/CVF Conference on Computer Vision and Pattern Recognition (CVPR)*, pages 11305–11315, 2022.
- [11] Junsong Chen, Chongjian Ge, Enze Xie, Yue Wu, Lewei Yao, Xiaozhe Ren, Zhongdao Wang, Ping Luo, Huchuan Lu, and Zhenguo Li. Pixart- σ : Weak-to-strong training of diffusion transformer for 4k text-to-image generation. In *European Conference on Computer Vision*, pages 74–91. Springer, 2024.
- [12] Junsong Chen, Jincheng Yu, Chongjian Ge, Lewei Yao, Enze Xie, Yue Wu, Zhongdao Wang, James Kwok, Ping Luo, Huchuan Lu, et al. Pixart- α : Fast training of diffusion transformer for photorealistic text-to-image synthesis. In *International Conference on Learning Representations*, 2024.
- [13] Xiaokang Chen, Zhiyu Wu, Xingchao Liu, Zizheng Pan, Wen Liu, Zhenda Xie, Xingkai Yu, and Chong Ruan. Janus-pro: Unified multimodal understanding and generation with data and model scaling. [arXiv preprint arXiv:2501.17811](https://arxiv.org/abs/2501.17811), 2025.
- [14] Zhe Chen, Weiyun Wang, Hao Tian, Shenglong Ye, Zhangwei Gao, Erfei Cui, Wenwen Tong, Kongzhi Hu, Jiapeng Luo, Zheng Ma, et al. How far are we to gpt-4v? closing the gap to commercial multimodal models with open-source suites. [Science China Information Sciences](https://doi.org/10.1007/s11432-024-22010-1), 67(12):220101, 2024.

[15] Wenliang Dai, Junnan Li, Dongxu Li, Anthony Tiong, Junqi Zhao, Weisheng Wang, Boyang Li, Pascale N Fung, and Steven Hoi. Instructblip: Towards general-purpose vision-language models with instruction tuning. *Advances in neural information processing systems*, 36:49250–49267, 2023.

[16] Chaorui Deng, Deyao Zhu, Kunchang Li, Chenhui Gou, Feng Li, Zeyu Wang, Shu Zhong, Weihao Yu, Xiaonan Nie, Ziang Song, et al. Emerging properties in unified multimodal pretraining. *arXiv preprint arXiv:2505.14683*, 2025.

[17] Haiwen Diao, Yufeng Cui, Xiaotong Li, Yueze Wang, Huchuan Lu, and Xinlong Wang. Unveiling encoder-free vision-language models. *Advances in Neural Information Processing Systems*, 37:52545–52567, 2024.

[18] Runpei Dong, Chunrui Han, Yuang Peng, Zekun Qi, Zheng Ge, Jinrong Yang, Liang Zhao, Jianjian Sun, Hongyu Zhou, Haoran Wei, et al. Dreamllm: Synergistic multimodal comprehension and creation. *arXiv preprint arXiv:2309.11499*, 2023.

[19] Patrick Esser, Robin Rombach, and Björn Ommer. Taming transformers for high-resolution image synthesis. *2021 IEEE/CVF Conference on Computer Vision and Pattern Recognition (CVPR)*, pages 12868–12878, 2020.

[20] Patrick Esser, Robin Rombach, and Björn Ommer. Taming transformers for high-resolution image synthesis. In *Proceedings of the IEEE/CVF conference on computer vision and pattern recognition*, pages 12873–12883, 2021.

[21] Patrick Esser, Robin Rombach, and Björn Ommer. Taming transformers for high-resolution image synthesis. In *Proceedings of the IEEE/CVF Conference on Computer Vision and Pattern Recognition (CVPR)*, pages 12873–12883, 2021.

[22] Patrick Esser, Sumith Kulal, Andreas Blattmann, Rahim Entezari, Jonas Müller, Harry Saini, Yam Levi, Dominik Lorenz, Axel Sauer, Frederic Boesel, et al. Scaling rectified flow transformers for high-resolution image synthesis. In *International Conference on Machine Learning*, 2024.

[23] Xianghong Fang, Litao Guo, Hengchao Chen, Yuxuan Zhang, Dingjie Song, Yexin Liu, Hao Wang, Harry Yang, Yuan Yuan, Qiang Sun, et al. Enhancing vector quantization with distributional matching: A theoretical and empirical study. *arXiv preprint arXiv:2506.15078*, 2025.

[24] Chaoyou Fu, Peixian Chen, Yunhang Shen, Yulei Qin, Mengdan Zhang, Xu Lin, Jinrui Yang, Xiawu Zheng, Ke Li, Xing Sun, Yunsheng Wu, Rongrong Ji, Caifeng Shan, and Ran He. Mme: A comprehensive evaluation benchmark for multimodal large language models, 2025. URL <https://arxiv.org/abs/2306.13394>.

[25] Samir Yitzhak Gadre, Gabriel Ilharco, Alex Fang, Jonathan Hayase, Georgios Smyrnis, Thao Nguyen, Ryan Marten, Mitchell Wortsman, Dhruva Ghosh, Jieyu Zhang, et al. Datacomp: In search of the next generation of multimodal datasets. *Advances in Neural Information Processing Systems*, 36:27092–27112, 2023.

[26] Shanghua Gao, Pan Zhou, Ming-Ming Cheng, and Shuicheng Yan. Mdtv2: Masked diffusion transformer is a strong image synthesizer. *arXiv preprint arXiv:2303.14389*, 2023.

[27] Yuying Ge, Sijie Zhao, Ziyun Zeng, Yixiao Ge, Chen Li, Xintao Wang, and Ying Shan. Making llama see and draw with seed tokenizer. *arXiv preprint arXiv:2310.01218*, 2023.

[28] Google Gemini2. Experiment with gemini 2.0 flash native image generation, 2025. URL <https://developers.googleblog.com/en/experiment-with-gemini-20-flash-native-image-generation/>.

[29] Dhruva Ghosh, Hannaneh Hajishirzi, and Ludwig Schmidt. Geneval: An object-focused framework for evaluating text-to-image alignment. *Advances in Neural Information Processing Systems*, 36:52132–52152, 2023.

[30] Yash Goyal, Tejas Khot, Douglas Summers-Stay, Dhruv Batra, and Devi Parikh. Making the v in vqa matter: Elevating the role of image understanding in visual question answering. In *Proceedings of the IEEE conference on computer vision and pattern recognition*, pages 6904–6913, 2017.

[31] Jian Han, Jinlai Liu, Yi Jiang, Bin Yan, Yuqi Zhang, Zehuan Yuan, Bingyue Peng, and Xiaobing Liu. Infinity: Scaling bitwise autoregressive modeling for high-resolution image synthesis. In *Proceedings of the Computer Vision and Pattern Recognition Conference*, pages 15733–15744, 2025.

[32] Martin Heusel, Hubert Ramsauer, Thomas Unterthiner, Bernhard Nessler, and Sepp Hochreiter. Gans trained by a two time-scale update rule converge to a local nash equilibrium. In *Neural Information Processing Systems*, 2017.

[33] Xiwei Hu, Rui Wang, Yixiao Fang, Bin Fu, Pei Cheng, and Gang Yu. Ella: Equip diffusion models with llm for enhanced semantic alignment. [arXiv preprint arXiv:2403.05135](#), 2024.

[34] Drew A Hudson and Christopher D Manning. Gqa: A new dataset for real-world visual reasoning and compositional question answering. In [Proceedings of the IEEE/CVF conference on computer vision and pattern recognition](#), pages 6700–6709, 2019.

[35] Aren Jansen, Daniel P. W. Ellis, Shawn Hershey, R. Channing Moore, Manoj Plakal, Ashok Popat, and Rif A. Saurous. Coincidence, categorization, and consolidation: Learning to recognize sounds with minimal supervision. [ICASSP 2020 - 2020 IEEE International Conference on Acoustics, Speech and Signal Processing \(ICASSP\)](#), pages 121–125, 2019.

[36] Mingkai Jia, Wei Yin, Xiaotao Hu, Jiaxin Guo, Xiaoyang Guo, Qian Zhang, Xiao-Xiao Long, and Ping Tan. Mgvq: Could vq-vae beat vae? a generalizable tokenizer with multi-group quantization. [arXiv preprint arXiv:2507.07997](#), 2025.

[37] Aniruddha Kembhavi, Mike Salvato, Eric Kolve, Minjoon Seo, Hannaneh Hajishirzi, and Ali Farhadi. A diagram is worth a dozen images. In [European conference on computer vision](#), pages 235–251. Springer, 2016.

[38] Diederik P. Kingma and Jimmy Ba. Adam: A method for stochastic optimization. [CoRR](#), abs/1412.6980, 2014.

[39] Diederik P. Kingma and Max Welling. Auto-encoding variational bayes. [CoRR](#), abs/1312.6114, 2013.

[40] Hugo Laurençon, Lucile Saulnier, Léo Tronchon, Stas Bekman, Amanpreet Singh, Anton Lozhkov, Thomas Wang, Siddharth Karamcheti, Alexander Rush, Douwe Kiela, et al. Obelics: An open web-scale filtered dataset of interleaved image-text documents. [Advances in Neural Information Processing Systems](#), 36:71683–71702, 2023.

[41] Doyup Lee, Chiheon Kim, Saehoon Kim, Minsu Cho, and Wook-Shin Han. Autoregressive image generation using residual quantization. In [Proceedings of the IEEE/CVF conference on computer vision and pattern recognition](#), pages 11523–11532, 2022.

[42] Bohao Li, Rui Wang, Guangzhi Wang, Yuying Ge, Yixiao Ge, and Ying Shan. Seed-bench: Benchmarking multimodal llms with generative comprehension. [arXiv preprint arXiv:2307.16125](#), 2023.

[43] Daiqing Li, Aleks Kamko, Ehsan Akhgari, Ali Sabet, Linmiao Xu, and Suhail Doshi. Playground v2. 5: Three insights towards enhancing aesthetic quality in text-to-image generation. [arXiv preprint arXiv:2402.17245](#), 2024.

[44] Junnan Li, Dongxu Li, Silvio Savarese, and Steven Hoi. Blip-2: Bootstrapping language-image pre-training with frozen image encoders and large language models. In [International conference on machine learning](#), pages 19730–19742. PMLR, 2023.

[45] Tianhong Li, Yonglong Tian, He Li, Mingyang Deng, and Kaiming He. Autoregressive image generation without vector quantization. In [NeurIPS](#), 2024.

[46] Xiang Li, Kai Qiu, Hao Chen, Jason Kuen, Jiuxiang Gu, Bhiksha Raj, and Zhe Lin. Imagefolder: Autoregressive image generation with folded tokens. [ArXiv](#), abs/2410.01756, 2024. URL <https://api.semanticscholar.org/CorpusID:273025912>.

[47] Yifan Li, Yifan Du, Kun Zhou, Jinpeng Wang, Wayne Xin Zhao, and Ji-Rong Wen. Evaluating object hallucination in large vision-language models. [arXiv preprint arXiv:2305.10355](#), 2023.

[48] Zhimin Li, Jianwei Zhang, Qin Lin, Jiangfeng Xiong, Yanxin Long, Xinchi Deng, Yingfang Zhang, Xingchao Liu, Minbin Huang, Zedong Xiao, et al. Hunyuan-dit: A powerful multi-resolution diffusion transformer with fine-grained chinese understanding. [arXiv preprint arXiv:2405.08748](#), 2024.

[49] Ji Lin, Hongxu Yin, Wei Ping, Pavlo Molchanov, Mohammad Shoeybi, and Song Han. Vila: On pre-training for visual language models. In [Proceedings of the IEEE/CVF conference on computer vision and pattern recognition](#), pages 26689–26699, 2024.

[50] Tsung-Yi Lin, Michael Maire, Serge J. Belongie, James Hays, Pietro Perona, Deva Ramanan, Piotr Dollár, and C. Lawrence Zitnick. Microsoft coco: Common objects in context. In [European Conference on Computer Vision](#), 2014. URL <https://api.semanticscholar.org/CorpusID:14113767>.

[51] Hao Liu, Wilson Yan, Matei Zaharia, and Pieter Abbeel. World model on million-length video and language with blockwise ringattention. [arXiv preprint arXiv:2402.08268](#), 2024.

[52] Haotian Liu, Chunyuan Li, Qingyang Wu, and Yong Jae Lee. Visual instruction tuning. *Advances in neural information processing systems*, 36:34892–34916, 2023.

[53] Haotian Liu, Chunyuan Li, Yuheng Li, and Yong Jae Lee. Improved baselines with visual instruction tuning. In *Proceedings of the IEEE/CVF conference on computer vision and pattern recognition*, pages 26296–26306, 2024.

[54] Haotian Liu, Chunyuan Li, Yuheng Li, Bo Li, Yuanhan Zhang, Sheng Shen, and Yong Jae. Lee. Llava-next: Improved reasoning, ocr, and world knowledge., 2024. URL <https://llava-vl.github.io/blog/2024-01-30-llava-next/>.

[55] Shiyu Liu, Yucheng Han, Peng Xing, Fukun Yin, Rui Wang, Wei Cheng, Jiaqi Liao, Yingming Wang, Honghao Fu, Chunrui Han, Guopeng Li, Yuang Peng, Quan Sun, Jingwei Wu, Yan Cai, Zheng Ge, Ranchen Ming, Lei Xia, Xianfang Zeng, Yibo Zhu, Binxing Jiao, Xiangyu Zhang, Gang Yu, and Dixin Jiang. Step1x-edit: A practical framework for general image editing. *arXiv preprint arXiv:2504.17761*, 2025.

[56] Shiyu Liu, Yucheng Han, Peng Xing, Fukun Yin, Rui Wang, Wei Cheng, Jiaqi Liao, Yingming Wang, Honghao Fu, Chunrui Han, et al. Step1x-edit: A practical framework for general image editing. *arXiv preprint arXiv:2504.17761*, 2025.

[57] Pan Lu, Swaroop Mishra, Tanglin Xia, Liang Qiu, Kai-Wei Chang, Song-Chun Zhu, Oyvind Tafjord, Peter Clark, and Ashwin Kalyan. Learn to explain: Multimodal reasoning via thought chains for science question answering. *Advances in Neural Information Processing Systems*, 35:2507–2521, 2022.

[58] Zhuoyan Luo, Fengyuan Shi, Yixiao Ge, Yujiu Yang, Limin Wang, and Ying Shan. Open-magvit2: An open-source project toward democratizing auto-regressive visual generation. *ArXiv*, abs/2409.04410, 2024.

[59] Zhuoyan Luo, Fengyuan Shi, Yixiao Ge, Yujiu Yang, Limin Wang, and Ying Shan. Open-magvit2: An open-source project toward democratizing auto-regressive visual generation. *arXiv preprint arXiv:2409.04410*, 2024.

[60] Chuofan Ma, Yi Jiang, Junfeng Wu, Jihan Yang, Xin Yu, Zehuan Yuan, Bingyue Peng, and Xiaojuan Qi. Unitok: A unified tokenizer for visual generation and understanding. *ArXiv*, abs/2502.20321, 2025.

[61] Chuofan Ma, Yi Jiang, Junfeng Wu, Jihan Yang, Xin Yu, Zehuan Yuan, Bingyue Peng, and Xiaojuan Qi. Unitok: A unified tokenizer for visual generation and understanding. *arXiv preprint arXiv:2502.20321*, 2025.

[62] Nanye Ma, Mark Goldstein, Michael S Albergo, Nicholas M Boffi, Eric Vanden-Eijnden, and Saining Xie. Sit: Exploring flow and diffusion-based generative models with scalable interpolant transformers. In *ECCV*, 2024.

[63] Ben Mann, Nick Ryder, Melanie Subbiah, J Kaplan, P Dhariwal, A Neelakantan, P Shyam, G Sastry, A Askell, S Agarwal, et al. Language models are few-shot learners. *arXiv preprint arXiv:2005.14165*, 1(3):3, 2020.

[64] Ahmed Masry, Xuan Long Do, Jia Qing Tan, Shafiq Joty, and Enamul Hoque. Chartqa: A benchmark for question answering about charts with visual and logical reasoning. In *Findings of the association for computational linguistics: ACL 2022*, pages 2263–2279, 2022.

[65] OpenAI. Introducing 4o image generation, 2025. URL <https://openai.com/index/introducing-4o-image-generation/>.

[66] Ziqi Pang, Tianyuan Zhang, Fujun Luan, Yunze Man, Hao Tan, Kai Zhang, William T Freeman, and Yu-Xiong Wang. Randar: Decoder-only autoregressive visual generation in random orders. In *CVPR*, 2025.

[67] William Peebles and Saining Xie. Scalable diffusion models with transformers. In *ICCV*, 2023.

[68] Dustin Podell, Zion English, Kyle Lacey, Andreas Blattmann, Tim Dockhorn, Jonas Müller, Joe Penna, and Robin Rombach. Sdxl: Improving latent diffusion models for high-resolution image synthesis. *arXiv preprint arXiv:2307.01952*, 2023.

[69] Liao Qu, Huichao Zhang, Yiheng Liu, Xu Wang, Yi Jiang, Yiming Gao, Hu Ye, Daniel K. Du, Zehuan Yuan, and Xinglong Wu. Tokenflow: Unified image tokenizer for multimodal understanding and generation. *2025 IEEE/CVF Conference on Computer Vision and Pattern Recognition (CVPR)*, pages 2545–2555, 2024. URL <https://api.semanticscholar.org/CorpusID:274465079>.

[70] Alec Radford, Karthik Narasimhan, Tim Salimans, Ilya Sutskever, et al. Improving language understanding by generative pre-training. 2018.

[71] Alec Radford, Jeffrey Wu, Rewon Child, David Luan, Dario Amodei, Ilya Sutskever, et al. Language models are unsupervised multitask learners. *OpenAI blog*, 1(8):9, 2019.

[72] Alec Radford, Jong Wook Kim, Chris Hallacy, Aditya Ramesh, Gabriel Goh, Sandhini Agarwal, Girish Sastry, Amanda Askell, Pamela Mishkin, Jack Clark, et al. Learning transferable visual models from natural language supervision. In *International conference on machine learning*, pages 8748–8763. PMLR, 2021.

[73] Robin Rombach, Andreas Blattmann, Dominik Lorenz, Patrick Esser, and Björn Ommer. High-resolution image synthesis with latent diffusion models. In *Proceedings of the IEEE/CVF conference on computer vision and pattern recognition*, pages 10684–10695, 2022.

[74] Robin Rombach, Andreas Blattmann, Dominik Lorenz, Patrick Esser, and Björn Ommer. High-resolution image synthesis with latent diffusion models. In *Proceedings of the IEEE/CVF conference on computer vision and pattern recognition*, pages 10684–10695, 2022.

[75] Olga Russakovsky, Jia Deng, Hao Su, Jonathan Krause, Sanjeev Satheesh, Sean Ma, Zhiheng Huang, Andrej Karpathy, Aditya Khosla, Michael S. Bernstein, Alexander C. Berg, and Li Fei-Fei. Imagenet large scale visual recognition challenge. *International Journal of Computer Vision*, 115:211 – 252, 2014.

[76] Kyle Sargent, Kyle Hsu, Justin Johnson, Li Fei-Fei, and Jiajun Wu. Flow to the mode: Mode-seeking diffusion autoencoders for state-of-the-art image tokenization. *arXiv preprint arXiv:2503.11056*, 2025.

[77] Fengyuan Shi, Zhuoyan Luo, Yixiao Ge, Yujiu Yang, Ying Shan, and Limin Wang. Scalable image tokenization with index backpropagation quantization. *arXiv preprint arXiv:2412.02692*, 2024.

[78] Fengyuan Shi, Zhuoyan Luo, Yixiao Ge, Yujiu Yang, Ying Shan, and Limin Wang. Scalable image tokenization with index backpropagation quantization, 2025.

[79] Amanpreet Singh, Vivek Natarajan, Meet Shah, Yu Jiang, Xinlei Chen, Dhruv Batra, Devi Parikh, and Marcus Rohrbach. Towards vqa models that can read. In *Proceedings of the IEEE/CVF conference on computer vision and pattern recognition*, pages 8317–8326, 2019.

[80] Wei Song, Yuran Wang, Zijia Song, Yadong Li, Haoze Sun, Weipeng Chen, Zenan Zhou, Jianhua Xu, Jiaqi Wang, and Kaicheng yu. Dualtoken: Towards unifying visual understanding and generation with dual visual vocabularies. *ArXiv*, abs/2503.14324, 2025. URL <https://api.semanticscholar.org/CorpusID:277104378>.

[81] Peize Sun, Yi Jiang, Shoufa Chen, Shilong Zhang, Bingyue Peng, Ping Luo, and Zehuan Yuan. Autoregressive model beats diffusion: Llama for scalable image generation. *ArXiv*, abs/2406.06525, 2024.

[82] Peize Sun, Yi Jiang, Shoufa Chen, Shilong Zhang, Bingyue Peng, Ping Luo, and Zehuan Yuan. Autoregressive model beats diffusion: Llama for scalable image generation. *arXiv preprint arXiv:2406.06525*, 2024.

[83] Quan Sun, Yufeng Cui, Xiaosong Zhang, Fan Zhang, Qiying Yu, Yueze Wang, Yongming Rao, Jingjing Liu, Tiejun Huang, and Xinlong Wang. Generative multimodal models are in-context learners. In *Proceedings of the IEEE/CVF Conference on Computer Vision and Pattern Recognition*, pages 14398–14409, 2024.

[84] Chameleon Team. Chameleon: Mixed-modal early-fusion foundation models. *arXiv preprint arXiv:2405.09818*, 2024.

[85] Chameleon Team. Chameleon: Mixed-modal early-fusion foundation models. *arXiv preprint arXiv:2405.09818*, 2024.

[86] NextStep Team, Chunrui Han, Guopeng Li, Jingwei Wu, Quan Sun, Yan Cai, Yuang Peng, Zheng Ge, Deyu Zhou, Haomiao Tang, et al. Nextstep-1: Toward autoregressive image generation with continuous tokens at scale. *arXiv preprint arXiv:2508.10711*, 2025.

[87] Keyu Tian, Yi Jiang, Zehuan Yuan, Bingyue Peng, and Liwei Wang. Visual autoregressive modeling: Scalable image generation via next-scale prediction. *ArXiv*, abs/2404.02905, 2024.

[88] Keyu Tian, Yi Jiang, Zehuan Yuan, Bingyue Peng, and Liwei Wang. Visual autoregressive modeling: Scalable image generation via next-scale prediction. 2024.

[89] Hugo Touvron, Thibaut Lavril, Gautier Izacard, Xavier Martinet, Marie-Anne Lachaux, Timothée Lacroix, Baptiste Rozière, Naman Goyal, Eric Hambro, Faisal Azhar, et al. Llama: Open and efficient foundation language models. *arXiv preprint arXiv:2302.13971*, 2023.

[90] Aaron Van Den Oord, Oriol Vinyals, et al. Neural discrete representation learning. *Advances in neural information processing systems*, 30, 2017.

[91] Chunwei Wang, Guansong Lu, Junwei Yang, Runhui Huang, Jianhua Han, Lu Hou, Wei Zhang, and Hang Xu. Illume: Illuminating your llms to see, draw, and self-enhance. In *Proceedings of the IEEE/CVF International Conference on Computer Vision*, pages 21612–21622, 2025.

[92] Junke Wang, Zhi Tian, Xun Wang, Xinyu Zhang, Weilin Huang, Zuxuan Wu, and Yu-Gang Jiang. Simplear: Pushing the frontier of autoregressive visual generation through pretraining, sft, and rl. *arXiv preprint arXiv:2504.11455*, 2025.

[93] Xinlong Wang, Xiaosong Zhang, Zhengxiong Luo, Quan Sun, Yufeng Cui, Jinsheng Wang, Fan Zhang, Yueze Wang, Zhen Li, Qiyi Yu, et al. Emu3: Next-token prediction is all you need. *arXiv preprint arXiv:2409.18869*, 2024.

[94] Xinlong Wang, Xiaosong Zhang, Zhengxiong Luo, Quan Sun, Yufeng Cui, Jinsheng Wang, Fan Zhang, Yueze Wang, Zhen Li, Qiyi Yu, et al. Emu3: Next-token prediction is all you need. *arXiv preprint arXiv:2409.18869*, 2024.

[95] Zhou Wang, Alan Conrad Bovik, Hamid R. Sheikh, and Eero P. Simoncelli. Image quality assessment: from error visibility to structural similarity. *IEEE Transactions on Image Processing*, 13:600–612, 2004.

[96] Zidong Wang, Lei Bai, Xiangyu Yue, Wanli Ouyang, and Yiyuan Zhang. Native-resolution image synthesis. *arXiv preprint arXiv:2506.03131*, 2025.

[97] Chengyue Wu, Xiaokang Chen, Zhiyu Wu, Yiyang Ma, Xingchao Liu, Zizheng Pan, Wen Liu, Zhenda Xie, Xingkai Yu, Chong Ruan, et al. Janus: Decoupling visual encoding for unified multimodal understanding and generation. In *Proceedings of the Computer Vision and Pattern Recognition Conference*, pages 12966–12977, 2025.

[98] Pingyu Wu, Kai Zhu, Yu Liu, Longxiang Tang, Jian Yang, Yansong Peng, Wei Zhai, Yang Cao, and Zheng-Jun Zha. Alitok: Towards sequence modeling alignment between tokenizer and autoregressive model. *arXiv preprint arXiv:2506.05289*, 2025.

[99] Sizhe Wu, Wenwei Zhang, Lumin Xu, Sheng Jin, Zhonghua Wu, Qingyi Tao, Wentao Liu, Wei Li, and Chen Change Loy. Harmonizing visual representations for unified multimodal understanding and generation. *arXiv preprint arXiv:2503.21979*, 2025.

[100] Yecheng Wu, Zhuoyang Zhang, Junyu Chen, Haotian Tang, Dacheng Li, Yunhao Fang, Ligeng Zhu, Enze Xie, Hongxu Yin, Li Yi, et al. Vila-u: a unified foundation model integrating visual understanding and generation. *arXiv preprint arXiv:2409.04429*, 2024.

[101] XAI. Realworldqa, 2024.

[102] Shitao Xiao, Yueze Wang, Junjie Zhou, Huaying Yuan, Xingrun Xing, Ruiran Yan, Chaofan Li, Shuting Wang, Tiejun Huang, and Zheng Liu. Omnigen: Unified image generation. *arXiv preprint arXiv:2409.11340*, 2024.

[103] Enze Xie, Junsong Chen, Yuyang Zhao, Jincheng Yu, Ligeng Zhu, Chengyue Wu, Yujun Lin, Zhekai Zhang, Muyang Li, Junyu Chen, et al. Sana 1.5: Efficient scaling of training-time and inference-time compute in linear diffusion transformer. *arXiv preprint arXiv:2501.18427*, 2025.

[104] Jinheng Xie, Weijia Mao, Zechen Bai, David Junhao Zhang, Weihao Wang, Kevin Qinghong Lin, Yuchao Gu, Zhijie Chen, Zhenheng Yang, and Mike Zheng Shou. Show-o: One single transformer to unify multimodal understanding and generation. *ArXiv*, abs/2408.12528, 2024.

[105] Jinheng Xie, Weijia Mao, Zechen Bai, David Junhao Zhang, Weihao Wang, Kevin Qinghong Lin, Yuchao Gu, Zhijie Chen, Zhenheng Yang, and Mike Zheng Shou. Show-o: One single transformer to unify multimodal understanding and generation. *arXiv preprint arXiv:2408.12528*, 2024.

[106] Tianwei Xiong, Jun Hao Liew, Zilong Huang, Jiashi Feng, and Xihui Liu. Gigatok: Scaling visual tokenizers to 3 billion parameters for autoregressive image generation, 2025.

[107] Qinghao Ye, Haiyang Xu, Jiabo Ye, Ming Yan, Anwen Hu, Haowei Liu, Qi Qian, Ji Zhang, and Fei Huang. mplug-owl2: Revolutionizing multi-modal large language model with modality collaboration. In *Proceedings of the ieee/cvf conference on computer vision and pattern recognition*, pages 13040–13051, 2024.

[108] Jiahui Yu, Xin Li, Jing Yu Koh, Han Zhang, Ruoming Pang, James Qin, Alexander Ku, Yuanzhong Xu, Jason Baldridge, and Yonghui Wu. Vector-quantized image modeling with improved vqgan. [arXiv preprint arXiv:2110.04627](https://arxiv.org/abs/2110.04627), 2021.

[109] Lijun Yu, Jose Lezama, Nitesh Bharadwaj Gundavarapu, Luca Versari, Kihyuk Sohn, David Minnen, Yong Cheng, Agrim Gupta, Xiuye Gu, Alexander G Hauptmann, et al. Language model beats diffusion-tokenizer is key to visual generation. In [ICLR](https://iclr.cc), 2024.

[110] Lijun Yu, José Lezama, Nitesh B. Gundavarapu, Luca Versari, Kihyuk Sohn, David Minnen, Yong Cheng, Vighnesh Birodkar, Agrim Gupta, Xiuye Gu, Alexander G. Hauptmann, Boqing Gong, Ming-Hsuan Yang, Irfan Essa, David A. Ross, and Lu Jiang. Language model beats diffusion – tokenizer is key to visual generation, 2024.

[111] Qifan Yu, Wei Chow, Zhongqi Yue, Kaihang Pan, Yang Wu, Xiaoyang Wan, Juncheng Li, Siliang Tang, Hanwang Zhang, and Yueteng Zhuang. Anyedit: Mastering unified high-quality image editing for any idea. [arXiv preprint arXiv:2411.15738](https://arxiv.org/abs/2411.15738), 2024.

[112] Qihang Yu, Mark Weber, Xueqing Deng, Xiaohui Shen, Daniel Cremers, and Liang-Chieh Chen. An image is worth 32 tokens for reconstruction and generation. [ArXiv](https://arxiv.org/abs/2406.07550), abs/2406.07550, 2024. URL <https://api.semanticscholar.org/CorpusID:270379986>.

[113] Qihang Yu, Mark Weber, Xueqing Deng, Xiaohui Shen, Daniel Cremers, and Liang-Chieh Chen. An image is worth 32 tokens for reconstruction and generation. [Advances in Neural Information Processing Systems](https://advances.neurips.cc), 37: 128940–128966, 2024.

[114] Qihang Yu, Ju He, Xueqing Deng, Xiaohui Shen, and Liang-Chieh Chen. Randomized autoregressive visual generation. In [ICCV](https://iccv.cc), pages 18431–18441, 2025.

[115] Sihyun Yu, Sangkyung Kwak, Huiwon Jang, Jongheon Jeong, Jonathan Huang, Jinwoo Shin, and Saining Xie. Representation alignment for generation: Training diffusion transformers is easier than you think. In [ICLR](https://iclr.cc), 2025.

[116] Xiang Yue, Yuansheng Ni, Kai Zhang, Tianyu Zheng, Ruoqi Liu, Ge Zhang, Samuel Stevens, Dongfu Jiang, Weiming Ren, Yuxuan Sun, et al. Mmmu: A massive multi-discipline multimodal understanding and reasoning benchmark for expert agi. In [Proceedings of the IEEE/CVF Conference on Computer Vision and Pattern Recognition](https://cvpr.cc), pages 9556–9567, 2024.

[117] Borui Zhang, Qihang Rao, Wenzhao Zheng, Jie Zhou, and Jiwen Lu. Quantize-then-rectify: Efficient vq-vae training. [arXiv preprint arXiv:2507.10547](https://arxiv.org/abs/2507.10547), 2025.

[118] Kai Zhang, Lingbo Mo, Wenhui Chen, Huan Sun, and Yu Su. Magicbrush: A manually annotated dataset for instruction-guided image editing. In [NeurIPS](https://neurips.cc), 2023.

[119] Richard Zhang, Phillip Isola, Alexei A. Efros, Eli Shechtman, and Oliver Wang. The unreasonable effectiveness of deep features as a perceptual metric. [2018 IEEE/CVF Conference on Computer Vision and Pattern Recognition](https://cvpr.cc), pages 586–595, 2018.

[120] Yue Zhao, Yuanjun Xiong, and Philipp Krahenbuhl. Image and video tokenization with binary spherical quantization. [ArXiv](https://arxiv.org/abs/2406.07548), abs/2406.07548, 2024.

[121] Yue Zhao, Yuanjun Xiong, and Philipp Krähenbühl. Image and video tokenization with binary spherical quantization. [arXiv preprint arXiv:2406.07548](https://arxiv.org/abs/2406.07548), 2024.

[122] Yue Zhao, Fuzhao Xue, Scott Reed, Linxi Fan, Yuke Zhu, Jan Kautz, Zhiding Yu, Philipp Krahenbuhl, and De-An Huang. Qlip: Text-aligned visual tokenization unifies auto-regressive multimodal understanding and generation. [ArXiv](https://arxiv.org/abs/2502.05178), abs/2502.05178, 2025.

[123] Anlin Zheng, Xin Wen, Xuanyang Zhang, Chuofan Ma, Tiancai Wang, Gang Yu, Xiangyu Zhang, and Xiaojuan Qi. Vision foundation models as effective visual tokenizers for autoregressive image generation. [arXiv preprint arXiv:2507.08441](https://arxiv.org/abs/2507.08441), 2025.

[124] Chunting Zhou, Lili Yu, Arun Babu, Kushal Tirumala, Michihiro Yasunaga, Leonid Shamis, Jacob Kahn, Xuezhe Ma, Luke Zettlemoyer, and Omer Levy. Transfusion: Predict the next token and diffuse images with one multi-modal model. [arXiv preprint arXiv:2408.11039](https://arxiv.org/abs/2408.11039), 2024.

[125] Lei Zhu, Fangyun Wei, Yanye Lu, and Dong Chen. Scaling the codebook size of vq-gan to 100,000 with a utilization rate of 99%. [Advances in Neural Information Processing Systems](https://advances.neurips.cc), 37:12612–12635, 2024.

- [126] Shaobin Zhuang, Yiwei Guo, Canmiao Fu, Zhipeng Huang, Zeyue Tian, Fangyikang Wang, Ying Zhang, Chen Li, and Yali Wang. Wetok: Powerful discrete tokenization for high-fidelity visual reconstruction. [arXiv preprint arXiv:2508.05599](https://arxiv.org/abs/2508.05599), 2025.
- [127] Shaobin Zhuang, Yiwei Guo, Canmiao Fu, Zhipeng Huang, Zeyue Tian, Fangyikang Wang, Ying Zhang, Chen Li, and Yali Wang. Wetok: Powerful discrete tokenization for high-fidelity visual reconstruction. [arXiv preprint arXiv:2508.05599](https://arxiv.org/abs/2508.05599), 2025.

Appendix

A Model Architecture

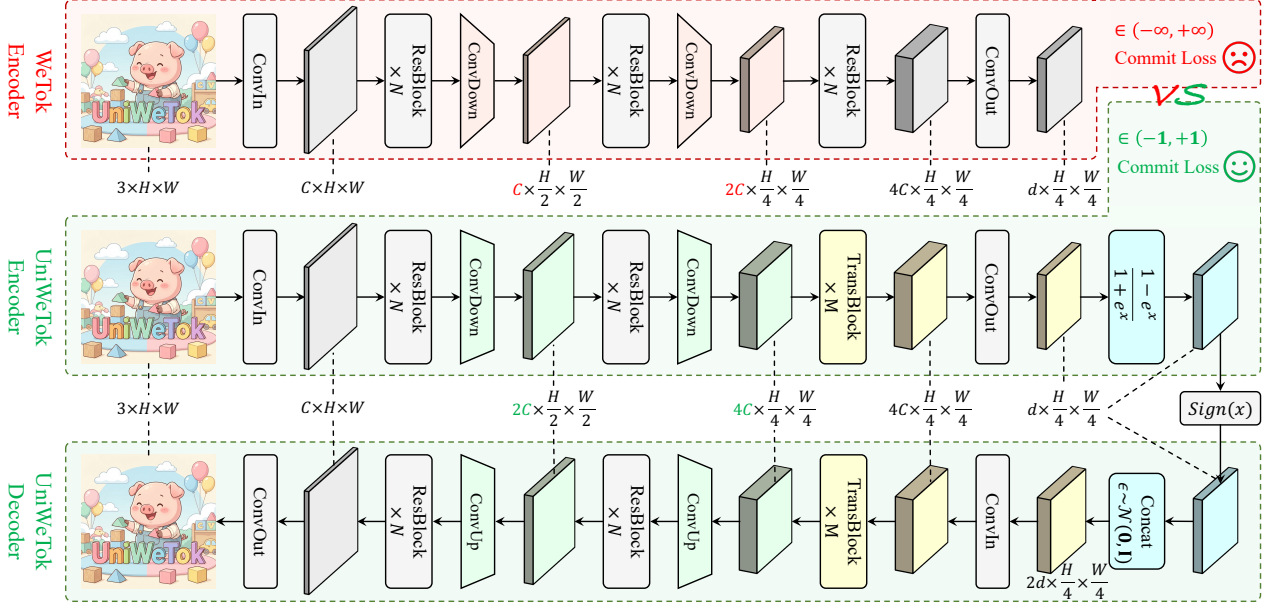


Figure 5 Detail Illustration of the UniWeTok model architecture.

B More Ablation Implementation Details

Training loss. As shown in Tab. 14, 15, 16.

SigLu activation. As shown in Tab. 17, 18, 19.

Pre-Post Distillation. As shown in Tab. 20, 21, 22.

Bottleneck channel. As shown in Tab. 23, 24.

Generative-Aware Prior. As shown in Tab. 25, 26, 27.

Training configurations on DataComp-1B. As shown in Tab. 28, 29, 30.

Hybrid architecture. As shown in Tab. 31, 32, 33.

BitDance-T. As detailed in Sec. 3 and 4, BitDance-T is an ultra-lightweight model with merely 8.6M parameters. Consequently, the additional computational overhead incurred during the training phase is negligible.

Inference. During the inference phase, the semantic teacher and generative prior model are not required. Consequently, UniWeTok relies solely on a single encoder and decoder.

C More Visualization Results

Multimodal Understanding. More visualization results of multimodal understanding by UniWeTok-Chat could be found in Fig. ??.

Image Editing. More visualization results of image editing by UniWeTok-Edit could be found in Fig. 7,8,9.

Table 14 w/o. PPD w/o. GAP setting.

config	w/o. PPD w/o. GAP
training data	IN-1K training set
image size	[256, 256]
data augmentation	random crop
downsample	32 × 32
ema	True
g (group number)	16
d' (group channel)	8
optimizer	Adam
optimizer momentum	$\beta_1, \beta_2=0.5, 0.9$
weight decay	0
learning rate schedule	consistent
learning rate	1e-4
warmup steps	0
cos decay end ratio	1
total steps	250250
channel_mult	[1,2,2,4,8]
channel	128
num_res_blocks	2
bottleneck channel double	True
num_attn_blocks	16
generative decoder	True
semantic teacher	—
SigLu activation	False
pre distillation	False
post distillation	False
distill head	linear
prior model	—
query token	False
global batchsize	128

Table 15 w/. PPD w/o. GAP setting.

config	w/. PPD w/o. GAP
training data	IN-1K training set
image size	[256, 256]
data augmentation	random crop
downsample	32 × 32
ema	True
g (group number)	16
d' (group channel)	8
optimizer	Adam
optimizer momentum	$\beta_1, \beta_2=0.5, 0.9$
weight decay	0
learning rate schedule	consistent
learning rate	1e-4
warmup steps	0
cos decay end ratio	1
total steps	250250
channel_mult	[1,1,2,2,4,8]
channel	128
num_res_blocks	2
bottleneck channel double	True
num_attn_blocks	16
generative decoder	True
semantic teacher	ViT-SO400M-16-SigLIP2-384
SigLu activation	True
pre distillation	True
post distillation	True
distill head	linear
prior model	—
query token	False
global batchsize	128

Table 16 w/. PPD w/. GAP setting.

config	w/. PPD w/. GAP
training data	IN-1K training set
image size	[256, 256]
data augmentation	random crop
downsample	32 × 32
ema	True
g (group number)	16
d' (group channel)	8
optimizer	Adam
optimizer momentum	$\beta_1, \beta_2=0.5, 0.9$
weight decay	0
learning rate schedule	consistent
learning rate	1e-4
warmup steps	0
cos decay end ratio	1
total steps	250250
channel_mult	[1,1,2,2,4,8]
channel	128
num_res_blocks	2
bottleneck channel double	True
num_attn_blocks	16
generative decoder	True
semantic teacher	ViT-SO400M-16-SigLIP2-384
SigLu activation	True
pre distillation	True
post distillation	True
distill head	linear
prior model	BitDance-T
query token	True
global batchsize	128

Table 17 Pre distillation setting.

config	pre distillation
training data	IN-1K training set
image size	[256, 256]
data augmentation	random crop
downsample	32 × 32
ema	True
g (group number)	16
d' (group channel)	8
optimizer	Adam
optimizer momentum	$\beta_1, \beta_2=0.5, 0.9$
weight decay	0
learning rate schedule	consistent
learning rate	1e-4
warmup steps	0
cos decay end ratio	1
total steps	250250
channel_mult	[1,1,2,2,4,8]
channel	128
num_res_blocks	2
bottleneck channel double	True
num_attn_blocks	16
generative decoder	True
semantic teacher	ViT-SO400M-16-SigLIP2-384
SigLu activation	False
pre distillation	True
post distillation	False
distill head	linear
prior model	—
query token	False
global batchsize	128

Table 18 Post distillation setting.

config	post distillation
training data	IN-1K training set
image size	[256, 256]
data augmentation	random crop
downsample	32 × 32
ema	True
g (group number)	16
d' (group channel)	8
optimizer	Adam
optimizer momentum	$\beta_1, \beta_2=0.5, 0.9$
weight decay	0
learning rate schedule	consistent
learning rate	1e-4
warmup steps	0
cos decay end ratio	1
total steps	250250
channel_mult	[1,1,2,2,4,8]
channel	128
num_res_blocks	2
bottleneck channel double	True
num_attn_blocks	16
generative decoder	True
semantic teacher	ViT-SO400M-16-SigLIP2-384
SigLu activation	False
pre distillation	False
post distillation	True
distill head	linear
prior model	—
query token	False
global batchsize	128

Table 19 Post distillation with SigLu activation setting.

config	post distillation with SigLu
training data	IN-1K training set
image size	[256, 256]
data augmentation	random crop
downsample	32 × 32
ema	True
g (group number)	16
d' (group channel)	8
optimizer	Adam
optimizer momentum	$\beta_1, \beta_2=0.5, 0.9$
weight decay	0
learning rate schedule	consistent
learning rate	1e-4
warmup steps	0
cos decay end ratio	1
total steps	250250
channel_mult	[1,1,2,2,4,8]
channel	128
num_res_blocks	2
bottleneck channel double	True
num_attn_blocks	16
generative decoder	True
semantic teacher	ViT-SO400M-16-SigLIP2-384
SigLu activation	True
pre distillation	False
post distillation	True
distill head	linear
prior model	—
query token	False
global batchsize	128

Table 20 Pre distillation setting.

config	pre distillation
training data	IN-1K training set
image size	[256, 256]
data augmentation	random crop
downsample	32 × 32
ema	True
g (group number)	16
d' (group channel)	8
optimizer	Adam
optimizer momentum	$\beta_1, \beta_2=0.5, 0.9$
weight decay	0
learning rate schedule	consistent
learning rate	1e-4
warmup steps	0
cos decay end ratio	1
total steps	250250
channel_mult	[1,1,2,2,4,8]
channel	128
num_res_blocks	2
bottleneck channel double	True
num_attn_blocks	16
generative decoder	True
semantic teacher	ViT-SO400M-16-SigLIP2-384
SigLu activation	True
pre distillation	True
post distillation	False
distill head	linear
prior model	—
query token	False
global batchsize	128

Table 21 Post distillation setting.

config	post distillation
training data	IN-1K training set
image size	[256, 256]
data augmentation	random crop
downsample	32 × 32
ema	True
g (group number)	16
d' (group channel)	8
optimizer	Adam
optimizer momentum	$\beta_1, \beta_2=0.5, 0.9$
weight decay	0
learning rate schedule	consistent
learning rate	1e-4
warmup steps	0
cos decay end ratio	1
total steps	250250
channel_mult	[1,1,2,2,4,8]
channel	128
num_res_blocks	2
bottleneck channel double	True
num_attn_blocks	16
generative decoder	True
semantic teacher	ViT-SO400M-16-SigLIP2-384
SigLu activation	True
pre distillation	False
post distillation	True
distill head	linear
prior model	—
query token	False
global batchsize	128

Table 22 Pre-Post distillation setting.

config	pre-post distillation
training data	IN-1K training set
image size	[256, 256]
data augmentation	random crop
downsample	32 × 32
ema	True
g (group number)	16
d' (group channel)	8
optimizer	Adam
optimizer momentum	$\beta_1, \beta_2=0.5, 0.9$
weight decay	0
learning rate schedule	consistent
learning rate	1e-4
warmup steps	0
cos decay end ratio	1
total steps	250250
channel_mult	[1,1,2,2,4,8]
channel	128
num_res_blocks	2
bottleneck channel double	True
num_attn_blocks	16
generative decoder	True
semantic teacher	ViT-SO400M-16-SigLIP2-384
SigLu activation	True
pre distillation	True
post distillation	True
distill head	linear
prior model	—
query token	False
global batchsize	128

Table 23 Single bottleneck channel setting.

config	single bottleneck channel
training data	IN-1K training set
image size	[256, 256]
data augmentation	random crop
downsample	32 × 32
ema	True
g (group number)	16
d' (group channel)	8
optimizer	Adam
optimizer momentum	$\beta_1, \beta_2=0.5, 0.9$
weight decay	0
learning rate schedule	consistent
learning rate	1e-4
warmup steps	0
cos decay end ratio	1
total steps	250250
channel_mult	[1,1,2,2,4,8]
channel	128
num_res_blocks	2
bottleneck channel double	False
num_attn_blocks	16
generative decoder	True
semantic teacher	ViT-SO400M-16-SigLIP2-384
SigLu activation	True
pre distillation	True
post distillation	True
distill head	linear
prior model	—
query token	False
global batchsize	128

Table 24 Double bottleneck channel setting.

config	double bottleneck channel
training data	IN-1K training set
image size	[256, 256]
data augmentation	random crop
downsample	32 × 32
ema	True
g (group number)	16
d' (group channel)	8
optimizer	Adam
optimizer momentum	$\beta_1, \beta_2=0.5, 0.9$
weight decay	0
learning rate schedule	consistent
learning rate	1e-4
warmup steps	0
cos decay end ratio	1
total steps	250250
channel_mult	[1,1,2,2,4,8]
channel	128
num_res_blocks	2
bottleneck channel double	True
num_attn_blocks	16
generative decoder	True
semantic teacher	ViT-SO400M-16-SigLIP2-384
SigLu activation	True
pre distillation	True
post distillation	True
distill head	linear
prior model	—
query token	False
global batchsize	128

Table 25 w/o. GAP w/o. Query setting.

config	w/o. GAP w/o. Query
training data	IN-1K training set
image size	[256, 256]
data augmentation	random crop
downsample	32 × 32
ema	True
g (group number)	16
d' (group channel)	8
optimizer	Adam
optimizer momentum	$\beta_1, \beta_2=0.5, 0.9$
weight decay	0
learning rate schedule	consistent
learning rate	1e-4
warmup steps	0
cos decay end ratio	1
total steps	250250
channel_mult	[1,1,2,2,4,8]
channel	128
num_res_blocks	2
bottleneck channel double	True
num_attn_blocks	16
generative decoder	True
semantic teacher	
SigLu activation	True
pre distillation	True
post distillation	True
distill head	linear
prior model	—
query token	False
global batchsize	128

Table 26 w/. GAP w/o. Query setting.

config	w/. GAP w/o. Query
training data	IN-1K training set
image size	[256, 256]
data augmentation	random crop
downsample	32 × 32
ema	True
g (group number)	16
d' (group channel)	8
optimizer	Adam
optimizer momentum	$\beta_1, \beta_2=0.5, 0.9$
weight decay	0
learning rate schedule	consistent
learning rate	1e-4
warmup steps	0
cos decay end ratio	1
total steps	250250
channel_mult	[1,1,2,2,4,8]
channel	128
num_res_blocks	2
bottleneck channel double	True
num_attn_blocks	16
generative decoder	True
semantic teacher	
SigLu activation	True
pre distillation	True
post distillation	True
distill head	linear
prior model	BitDance-T
query token	False
global batchsize	128

Table 27 w/. GAP w/. Query setting.

config	w/. GAP w/. Query
training data	IN-1K training set
image size	[256, 256]
data augmentation	random crop
downsample	32 × 32
ema	True
g (group number)	16
d' (group channel)	8
optimizer	Adam
optimizer momentum	$\beta_1, \beta_2=0.5, 0.9$
weight decay	0
learning rate schedule	consistent
learning rate	1e-4
warmup steps	0
cos decay end ratio	1
total steps	250250
channel_mult	[1,1,2,2,4,8]
channel	128
num_res_blocks	2
bottleneck channel double	True
num_attn_blocks	16
generative decoder	True
semantic teacher	
SigLu activation	True
pre distillation	True
post distillation	True
prior model	BitDance-T
query token	True
global batchsize	128

Table 28 Linear head with batch-size 128 setting.

config	linear head with bs128
training data	DataComp-1B
image size	[256, 256]
data augmentation	random crop
downsample	32 × 32
ema	True
g (group number)	16
d' (group channel)	8
optimizer	Adam
optimizer momentum	$\beta_1, \beta_2=0.5, 0.9$
weight decay	0
learning rate schedule	consistent
learning rate	1e-4
warmup steps	0
cos decay end ratio	1
total steps	250250
channel_mult	[1,1,2,2,4,8]
channel	128
num_res_blocks	2
bottleneck channel double	True
num_attn_blocks	0
generative decoder	True
semantic teacher	
SigLu activation	True
pre distillation	True
post distillation	True
distill head	linear
prior model	BitDance-T
query token	True
global batchsize	128

Table 29 Attention head with batchsize 128 setting.

config	attention head with bs1024
training data	DataComp-1B
image size	[256, 256]
data augmentation	random crop
downsample	32 × 32
ema	True
g (group number)	16
d' (group channel)	8
optimizer	Adam
optimizer momentum	$\beta_1, \beta_2=0.5, 0.9$
weight decay	0
learning rate schedule	consistent
learning rate	1e-4
warmup steps	0
cos decay end ratio	1
total steps	250250
channel_mult	[1,1,2,2,4,8]
channel	128
num_res_blocks	2
bottleneck channel double	True
num_attn_blocks	0
generative decoder	True
semantic teacher	
SigLu activation	True
pre distillation	True
post distillation	True
distill head	attention
prior model	BitDance-T
query token	True
global batchsize	128

Table 30 Attention head with batchsize 1024 setting.

config	attention head with bs1024
training data	DataComp-1B
image size	[256, 256]
data augmentation	random crop
downsample	32 × 32
ema	True
g (group number)	16
d' (group channel)	8
optimizer	Adam
optimizer momentum	$\beta_1, \beta_2=0.5, 0.9$
weight decay	0
learning rate schedule	consistent
learning rate	1e-4
warmup steps	0
cos decay end ratio	1
total steps	250250
channel_mult	[1,1,2,2,4,8]
channel	128
num_res_blocks	2
bottleneck channel double	True
num_attn_blocks	0
generative decoder	True
semantic teacher	
SigLu activation	True
pre distillation	True
post distillation	True
distill head	attention
prior model	BitDance-T
query token	True
global batchsize	1024

Table 31 CNN architecture setting.

config	CNN architecture
training data	DataComp-1B
image size	[256, 256]
data augmentation	random crop
downsample	32 × 32
ema	True
g (group number)	16
d' (group channel)	8
optimizer	Adam
optimizer momentum	$\beta_1, \beta_2=0.5, 0.9$
weight decay	0
learning rate schedule	consistent
learning rate	1e-4
warmup steps	0
cos decay end ratio	1
total steps	250250
channel_mult	[1,1.2,2.4,8]
channel	128
num_res_blocks	2
bottleneck channel double	True
num_attn_blocks	0
generative decoder	True
semantic teacher	ViT-SO400M-16-SigLIP2-384
SigLu activation	True
pre distillation	True
post distillation	True
distill head	attention
prior model	BitDance-T
query token	True
global batchsize	1024

Table 32 Transformer architecture setting.

config	transformer architecture
training data	DataComp-1B
image size	[256, 256]
data augmentation	random crop
downsample	32 × 32
ema	True
g (group number)	16
d' (group channel)	8
optimizer	Adam
optimizer momentum	$\beta_1, \beta_2=0.5, 0.9$
weight decay	0
learning rate schedule	consistent
learning rate	1e-4
warmup steps	0
cos decay end ratio	1
total steps	250250
channel_mult	[1,1.2,2.4,8]
channel	128
num_res_blocks	0
bottleneck channel double	True
num_attn_blocks	16
generative decoder	True
semantic teacher	ViT-SO400M-16-SigLIP2-384
SigLu activation	True
pre distillation	True
post distillation	True
distill head	attention
prior model	BitDance-T
query token	True
global batchsize	1024

Table 33 Hybrid architecture setting.

config	hybrid architecture
training data	DataComp-1B
image size	[256, 256]
data augmentation	random crop
downsample	32 × 32
ema	True
g (group number)	16
d' (group channel)	8
optimizer	Adam
optimizer momentum	$\beta_1, \beta_2=0.5, 0.9$
weight decay	0
learning rate schedule	consistent
learning rate	1e-4
warmup steps	0
cos decay end ratio	1
total steps	250250
channel_mult	[1,1.2,2.4,8]
channel	128
num_res_blocks	2
bottleneck channel double	True
num_attn_blocks	16
generative decoder	True
semantic teacher	ViT-SO400M-16-SigLIP2-384
SigLu activation	True
pre distillation	True
post distillation	True
distill head	attention
prior model	BitDance-T
query token	True
global batchsize	1024

Image Caption



Please describe this image in detail.



The image depicts a peaceful indoor scene featuring an orange tabby cat sleeping soundly on a white windowsill. Outside the window, a bright blue sky with fluffy white clouds is visible. Sunlight streams through the glass, illuminating the cat's fur and creating a warm, cozy atmosphere.

OCR



What is written on the board?



The text on the board reads: "Daily Special: Coffee \$3 Cake \$4

ScienceQA



According to the diagram, what gas is released by the plant during this process? Choices: A. Carbon Dioxide B. Oxygen C. Nitrogen D. Hydrogen



Based on the diagram, the plant takes in sunlight and water to perform photosynthesis. The arrow pointing away from the leaf indicates the release of a byproduct. In photosynthesis, plants release Oxygen. Therefore, the correct answer is B.

TableQA

Item	Price	Stock
Mouse	\$20	50
Keyboard	\$40	30
Monitor	\$150	10



If a customer buys 2 Mice and 1 Keyboard, how much will they spend in total?

To calculate the total cost:

1. Price of a Mouse: \$20.
Quantity: 2. Cost: $\$20 \times 2 = \40 .
2. Price of a Keyboard: \$40.
Quantity: 1. Cost: $\$40 \times 1 = \40 .
3. Total: $\$40 + \$40 = \$80$. The customer will spend a total of \$80.

Figure 6 Visualization results of multimodal understanding by UniWeTok-Chat.

Input	Chinese Prompt Output	English Prompt Output
把背景换成海洋 / Adjust the background to the ocean		
背景换成星空 / Change the background to a starry sky		
将伞的颜色改为棕色 / Change the color of umbrellas to brown		
大象的颜色改为粉色 / Change the color of elephant to pink		

Figure 7 Visualization results of image editing by UniWeTok-Edit part 1.

Input	Chinese Prompt Output	English Prompt Output
<p>把床单颜色改为天蓝色 / Change the bed sheet color to sky blue</p>		
<p>将时钟的颜色改为棕色 / Alter the color of clocks to brown</p>		
<p>将大象的材质改为砖块 / Construct the elephant from bricks</p>		
<p>将图像风格替换为奇幻艺术 / Replace the image style with fantasy art</p>		

Figure 8 Visualization results of image editing by UniWeTok-Edit part 2.

Input	Chinese Prompt Output	English Prompt Output
	<i>做成油画风格. / Make it an oil painting</i>	
	<i>擦除斑马 / Erase the zebra</i>	
	<i>擦除砧板上的刀 / Erase the knife on the cutting board</i>	

Figure 9 Visualization results of image editing by UniWeTok-Edit part 3.